Transportation Research Part C 121 (2020) 102875

Contents lists available at ScienceDirect

Transportation Research Part C

journal homepage: www.elsevier.com/locate/trc

# Traffic synchronization in terminal airspace to enable continuous descent operations in trombone sequencing and merging procedures: An implementation study for Frankfurt airport

Raúl Sáez [a,*], Xavier Prats [a], Tatiana Polishchuk [b], Valentin Polishchuk [b]

[a] Technical University of Catalonia – BarcelonaTech, Department of Physics - Aerospace Engineering Division, Castelldefels, Spain
[b] Communications and Transport Systems, ITN, Linköping University, Norrköping, Sweden

ARTICLE INFO

*Keywords:*
Air traffic management
Traffic synchronization
Continuous descent operations
Required time of arrival
Trajectory optimization
Tromboning

ABSTRACT

This paper proposes to enhance the current tromboning paradigm with a four dimensional trajectory negotiation and synchronization process with the aim to maximise the number of neutral Continuous descent operations (CDOs, descents with idle thrust and no speed-brakes usage) achieved by the arriving traffic in terminal maneuvering areas (TMAs). An optimal control problem has been formulated and solved in order to generate a set of candidate CDO trajectories per aircraft, while a mixed-integer-linear programming model has been built in order to optimally assign routes of the arrival procedure and required times of arrival (RTAs) to the arriving traffic when still in cruise. The assessment has been performed for Frankfurt am Main airport (Germany), by using arrival traffic gathered from historical data. Results show that, after assigning an RTA and a route to every arriving aircraft, it is possible to maximize the number of aircraft performing CDOs while ensuring a safe time separation throughout the arrival procedure. For low traffic scenarios, the totality of traffic can be successfully scheduled, while for high traffic scenarios this is not the case and not all aircraft can be scheduled if neutral CDOs are flown. However, by assuming different arbitrarily defined arrival times to the TMA or by considering more additional shortcuts in the trombone procedure it is possible to increase the number of aircraft scheduled. Besides improving current operations in the short-mid term, the methodology presented in this paper could become a technical enabler towards a fully deployed trajectory based operations (TBO) environment.

## 1. Introduction

A continuously growing environmental sensitivity in aviation has encouraged the research into methods for achieving a greener air transportation. Continuous descent operations (CDOs) allow aircraft to follow an optimum flight path that delivers major environmental and economic benefits, giving engine-idle descents as a result that reduce fuel consumption, pollutant emissions and noise nuisance (Erkelens, 2000; Warren and Tong, 2002; Clarke et al., 2004).

CDOs are optimized to the operating capability of the aircraft, resulting in different optimum trajectories for aircraft with different characteristics. As a result, the vertical and time predictability of incoming traffic flows decreases, which leads to an increase of the air

* Corresponding author.
*E-mail addresses:* raul.saez.garcia@upc.edu (R. Sáez), xavier.prats@upc.edu (X. Prats), tatiana.polishchuk@liu.se (T. Polishchuk), valentin.polishchuk@liu.se (V. Polishchuk).

https://doi.org/10.1016/j.trc.2020.102875
Received 25 February 2020; Received in revised form 29 October 2020; Accepted 30 October 2020

traffic controller officer (ATCO) workload. Consequently, ATCOs would increase separation buffers leading to airspace and runway capacity losses that are not desirable in major terminal maneuvering areas (TMAs), especially during peak hours.

For the reasons stated above, in busy TMAs CDOs hardly take place. Firstly, and at a strategic level, altitude and speed constraints published in standard terminal arrival route (STAR) charts do not take into account the particular operating capability of each aircraft, thus limiting the possibility of performing optimum descent trajectories. Moreover, in the tactical level, ATCOs use instructions such as altitude assignments, speed adjustments and path stretching (i.e. radar vectoring, also called *open-loop* instructions) so as to maintain safe separation between aircraft and maximize the throughput. These techniques, however, tend to degrade the performance of descent operations, leading to a higher environmental impact. Furthermore, the duration of such open-loop vector instructions is not known by the aircraft crew, nor how the aircraft will re-join its initial route. As a result, it is impossible for state-of-the art flight management systems (FMS) to predict the remaining distance to go and, therefore, to optimize the trajectory to achieve the most environmentally-friendly descent profile. In order to address these issues, the International Civil Aviation Organization (ICAO) has published some CDO guidance material (ICAO, 2010) used to support air navigation service providers (ANSP) to design vertical corridors in which all descent trajectories must be contained, helping to strategically separate them from other procedures in the vicinity. However, as reported in Fricke et al. (2015), these criteria have been established without explicitly considering the aircraft type, assuming international standard atmosphere (ISA) conditions and with coarse assumptions regarding the aircraft gross mass and performance data. This leads, in the majority of cases, to too restrictive corridors that limit the potential CDO adherence in real operations.

Conversely, new air traffic management (ATM) paradigms such as the trajectory based operations (TBO) defined by SESAR (SESAR Joint Undertaking, 2015) or NextGen (Federal Aviation Administration, 2019), aim to completely remove open-loop vectoring and strategic constraints on the trajectories by efficiently implementing a four dimensional (4D) trajectory negotiation process to synchronize airborne and ground equipment with the aim of maximizing both flight efficiency and throughput. In this scenario, there would be no need for vectoring except for unforeseen or contingency situations.

An interim solution towards the full TBO concept consists in sequencing and merging arrival traffic by assigning required times of arrival (RTAs) at one or several fixes along a known route (2D trajectory). This allows the FMS to know the remaining distance to go, and thus, enable the aircraft to fly an optimal descent profile while satisfying the RTA (Klooster et al., 2009). Nevertheless, for high traffic loads it could be impossible to accommodate all the incoming traffic by only assigning RTAs (Pawełek et al., 2019). In those situations, the aircraft route should also be stretched to absorb even more delay.

Point merge and tromboning are two other interim strategies that lie in between full 4D negotiated trajectories and open-loop vectoring. Both methodologies have proven successful to maximize runway throughput, reduce ATCO workload and enhance significantly the aircraft crew situational awareness, since the predictability of the trajectory improves.

In a point merge arrival, aircraft fly sequencing legs at a constant altitude (typically between FL90 and FL110), until “direct to” instructions are given to a merge point, used for traffic integration (Ivanescu et al., 2009; Boursier et al., 2007). Its environmental benefits, however, are limited to altitudes below the sequencing leg altitude, since the remaining distance is known with certainty only after the “direct to” instruction. Thus, even if the CDO were initiated at the cruise level, it would be interrupted to maintain level flight while following the sequencing leg before cleared to the merge point, leading to an increase in fuel burn while leveling off at relatively low altitudes.

Regarding tromboning, in Sprong et al. (2005) it is demonstrated how this kind of procedures reduce lateral dispersion, time flown and distance flown, while at the same time allow arriving flights to remain at higher altitudes.

This paper proposes to enhance the current tromboning paradigm with a 4D trajectory negotiation and synchronization process with the aim to enable the highest number of neutral CDOs (descents with idle thrust and no speed-brakes usage); and to maximize runway throughput. It is assumed that an RTA and a route in the arrival procedure (which includes the trombone procedure) will be negotiated way before the top of descent in order to derive a 4D conflict free trajectory throughout the whole descent. Besides improving current operations in the short-mid term, the methodology presented in this paper could become a technical enabler towards enhanced arrival managers (AMAN) or advanced 4D trajectory synchronization technologies in line with the TBO paradigm.

To the best of the authors’ knowledge, no other works analyzed a high-demand scenario with real traffic, in which aircraft fly neutral CDOs from cruise level to a given metering fix by following a real trombone procedure in which separation is ensured at all waypoints. There are other works that proposed arrival schedulers with RTAs to manage all the incoming traffic; however, they assume fixed arrival routes (Sadovsky and Windhorst, 2019) or they do not necessarily enforce the use of CDOs (Zelinksi and Jung, 2015; Sadovsky and Windhorst, 2019). A small proof of concept was presented in a previous work by the authors (Sáez et al., 2018), but several limitations were present that are now addressed in this paper: mainly, time separation was not ensured in the entire procedure, as only the time windows in the metering fix were considered for the scheduling process, disregarding the rest of the waypoints. In addition, the RTA and route assignment were performed in two separate steps, instead of being both part of the output of the same scheduling algorithm. Furthermore, only low traffic scenarios were assessed in the initial proof of concept.

## 2. Concept of operations and methodology

This section details the methodology followed in this paper to solve the aircraft scheduling and synchronization problem in TMA, without open-loop instructions, by taking advantage of the tromboning philosophy. First of all, a brief description of trombone procedures is given in Section 2.1. Then, Section 2.2 describes the concept of operations proposed in this work, while Section 2.3 details the proposed method to assign a profile to the arriving aircraft. A profile has to be understood as the resulting descent trajectory when combining the assignment of an RTA and a route choice in the tromboning procedure. Finally, Section 2.4 presents the methodology used to generate the (optimal) trajectories for the validation scenarios of this paper (simulated traffic). In real life, these trajectories

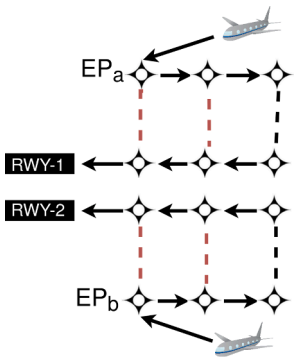


**Fig. 1.** Simplified diagram of a tromboning procedure.

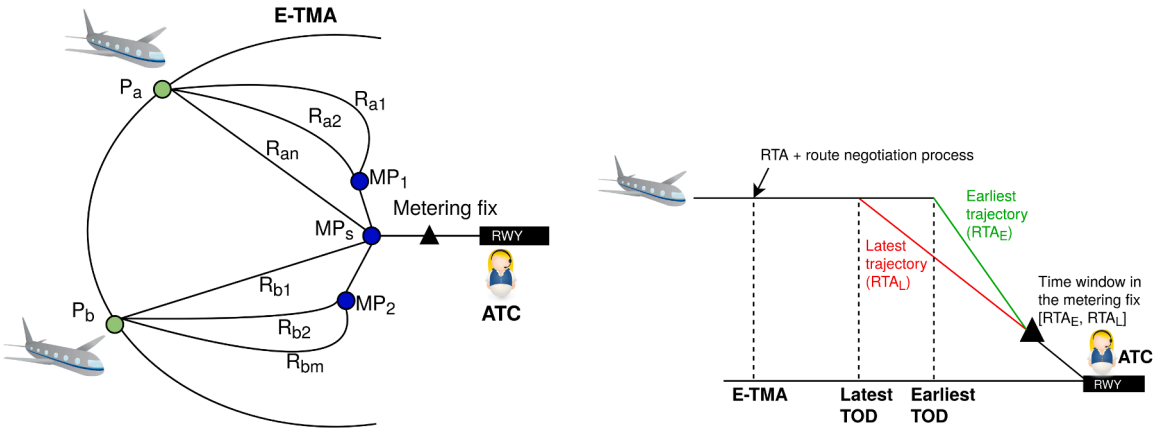


(a) Lateral perspective (b) Vertical perspective

**Fig. 2.** Concept of operations: trajectories.

would be generated by an advanced functionality of the FMS of each aircraft, equipped with the RTA functionality.

### 2.1. Tromboning procedures

Tromboning is a trombone-shape RNAV (area navigation) procedure consisting of a set of parallel legs composed of multiple waypoints, in which ATCOs may give a shortcut (depending on the traffic) to the next leg. Fig. 1 shows a simplified tromboning procedure, with two entry points ($EP_a$ and $EP_b$) for two different traffic flows. Aircraft are supposed to fly the full route (black lines in the figure) unless the ATC gives a shortcut at some of the waypoints. In such a case, aircraft would be able to fly one of the red-dashed trombone shortcuts depicted in the figure, which would suppose a reduction in the total distance flown. Currently, trombone procedures are used in several European airports, such as Munich and Frankfurt airports, in Germany, or Warsaw Chopin airport, in Poland. Recently, tromboning procedures have been implemented also in Barcelona-El Prat airport.

### 2.2. Concept of operations

Fig. 2 depicts a simplified scenario used to illustrate the problem addressed in this work. Suppose several aircraft trying to land in a given airport divided into N traffic flows of one or more aircraft each, entering an extended TMA (E-TMA) through several entry points ($P_a$ and $P_b$ in this case). In this paper we use the E-TMA nomenclature to emphasize the fact that the aircraft are still in the en-route phase of the flight when the sequencing requirements in the TMA are negotiated, which will include a revision of the trajectory's top of descent (TOD). In the majority of conventional TMAs, however, this would not be possible. TMAs are areas of controlled airspace surrounding the airport, designed to efficiently manage all the incoming and departing traffic. The size of a TMA depends on the level of traffic for which it is designed, so it will be bigger for airports with high traffic loads and smaller for airports with low traffic loads. In the case of small airports, it might even be designed up to altitudes below the top of descent of the majority of flights, which would mean that aircraft would be already descending. On the other hand, for big airports the aircraft may still be in cruise when entering the TMA; however, in most cases, there would not be enough time to efficiently negotiate the sequencing requirements with the ATC. In Europe, for instance, for some big airports such as Barcelona, the TMA horizontal limits are defined by the border with neighboring

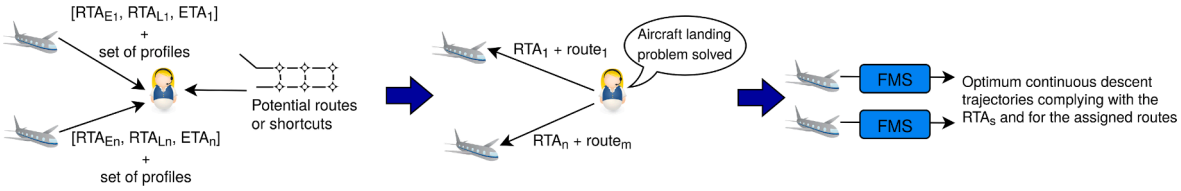


**Fig. 3.** Concept of operations: RTA and route negotiation process.

countries (in this case, by the border with France), leading to a loss of efficiency.

For each entry point, there are several available routes an aircraft could fly. These traffic flows could merge at several merging points ($MP_1 \ldots MP_s$), until they all meet at the metering fix, which is the point where the RTA will be assigned.

Once the aircraft enter the E-TMA, they start an RTA and route negotiation/synchronization process with the ATCO (or ground automated system), as shown in Fig. 3. First of all, aircraft are requested to compute their arrival time window in the metering fix, which is the difference between the earliest and the latest time of arrival at that fix ($RTA_E$ and $RTA_L$), which are assumed to be computed by the FMS of the different incoming aircraft by considering the earliest and latest trajectories (Fig. 2(b))[1]. In addition, the aircraft FMS downlink to the ATCO the aircraft estimated time of arrival and a set of finite profiles within the available time window (computed by the FMS too). It should be noted that, while the earliest and latest times of arrival at the metering fix will mainly depend on aircraft performance, flight envelope and weather conditions; the estimated time of arrival at the same fix will be obtained after computing the optimal descent trajectory for that particular flight, subject to airline and crew policies, such as the Cost Index setting for that particular flight[2]. It is worth highlighting the fact that the profiles are computed by on-board systems (such as an FMS), and not by ground systems, thus improving the accuracy of the generated trajectories as aircraft systems have access to much more accurate aircraft performance data.

After receiving all the profiles and analyzing the potential routes for each aircraft, ATCOs (with the help of an automated ground system) can solve the aircraft landing problem. They assign a profile (i.e. an RTA within each aircraft feasible time window and a route in the arrival procedure) to each aircraft that ensures a safe separation between aircraft throughout the whole arrival procedure (no matter how many routes and merging points) and which minimizes the deviation with respect to the aircraft estimated time of arrival at the metering fix. The objective is that the aircraft know this information while still in cruise, just after entering the E-TMA. Therefore, the FMS on-board can compute the neutral trajectory (i.e. idle thrust and no speebrakes usage) that complies with the RTA and follows the requested route by the ATCO.

One interesting matter is the width of the time window in the metering fix, which depends on several factors, e.g. the aircraft performance, weather conditions, etc. However, there are two factors that could be changed in order to obtain wider or shorter time windows. The first one is the type of CDO being considered. Neutral CDOs assume idle thrust and no speed-brakes usage throughout the descent, and are the ones considered in this work. Then, non-neutral or powered CDOs allow the use of thrust and speed-brakes, supposing a higher flexibility with respect to neutral CDOs, which leads to wider time windows, but at the expense of increasing the fuel burn and/or noise nuisance.

The other influential factor is related to the time when the RTA and route assignment are notified to the aircraft. If the ATCO sends this information when the aircraft enters the E-TMA while it is still in cruise, the time window will be wider than if the RTA and route are assigned while the aircraft is already descending. While in cruise, the aircraft could accelerate or decelerate to achieve earlier or later times of arrival. Furthermore, the position of the TOD can be changed too. Several studies have dealt with the assignment of RTAs (and the quantification of the feasible time window) when the aircraft is still in cruise, well before the top of descent (TOD). The work presented in Takeichi and Inami (2010) quantified the feasible time window that could be achieved by either enabling the addition (resp. omission) of waypoints to stretch (resp. reduce) the flight path length, or adjusting the duration of the cruise phase. However, as it has been aforementioned, ATCOs could potentially assign or update previously assigned RTAs while the aircraft is already descending. This is addressed in Dalmau and Prats (2017), where it is shown that the available time window allowing to update the RTA while still executing a CDO at idle thrust is in some cases still significant.

Ideally, the RTA and route negotiation/synchronization process should be done as soon as aircraft enter the E-TMA. However, this would be feasible only if the flight sequence is generated fast enough so that aircraft know the profiles they have been assigned before reaching the TOD. Otherwise, the communication between the aircraft and the ATC should be established before the E-TMA, with enough look-ahead time to make the required computations.

### 2.3. Aircraft landing problem

The goal of the aircraft landing problem considered in this paper is to schedule the arrival traffic to the E-TMA by assigning one

[1] The top of descent for the earliest trajectory is further (or closer to the metering fix) than the top of descent for the latest trajectory, as aircraft can fly at higher speeds during the cruise phase (Fig. 7).

[2] The Cost Index is a parameter chosen by the airspace user that reflects the relative importance of the cost of time with respect to fuel costs (Airbus, 1998).

profile to each aircraft $a$. This involves assigning both RTAs at the metering fix and routes to all incoming traffic. Each RTA must fit within the corresponding feasible time window for each particular aircraft and, together with the route assignment, a time separation between aircraft must be ensured through the whole descent. As commented before, this feasible time window, together with the estimated time of arrival at the metering fix $ETA_a$, is assumed to be computed by the FMS of each aircraft and down-linked, as input, to the aircraft landing scheduler.

In this work, the arrival time window in the metering fix is discretized. This leads to a finite set of candidate descent profiles per aircraft, which are also computed by the FMS and down-linked to the aircraft landing scheduler. The process followed in order to solve the aircraft landing problem and, thus, to obtain an optimal profile assignment, is shown in Fig. 4 and detailed below:

1. The possible routes for each aircraft arriving to the destination airport are obtained from the arrival and approach charts published by the corresponding country's AIP (aeronautical information publication). Each route is discretized in a finite number of segments, so that new (intermediate) waypoints are added to the procedure.
2. By observing the arriving traffic and the airport arrival procedure the entry points for each incoming aircraft are obtained, which are those corresponding to the moment the aircraft enters the E-TMA. As soon as aircraft enter this area, the RTA and route negotiation process starts.
3. The FMS of each aircraft computes a set of candidate profiles. These profiles are computed per route and thus, the arrival time windows at the metering fix (for each aircraft and possible route) are obtained.

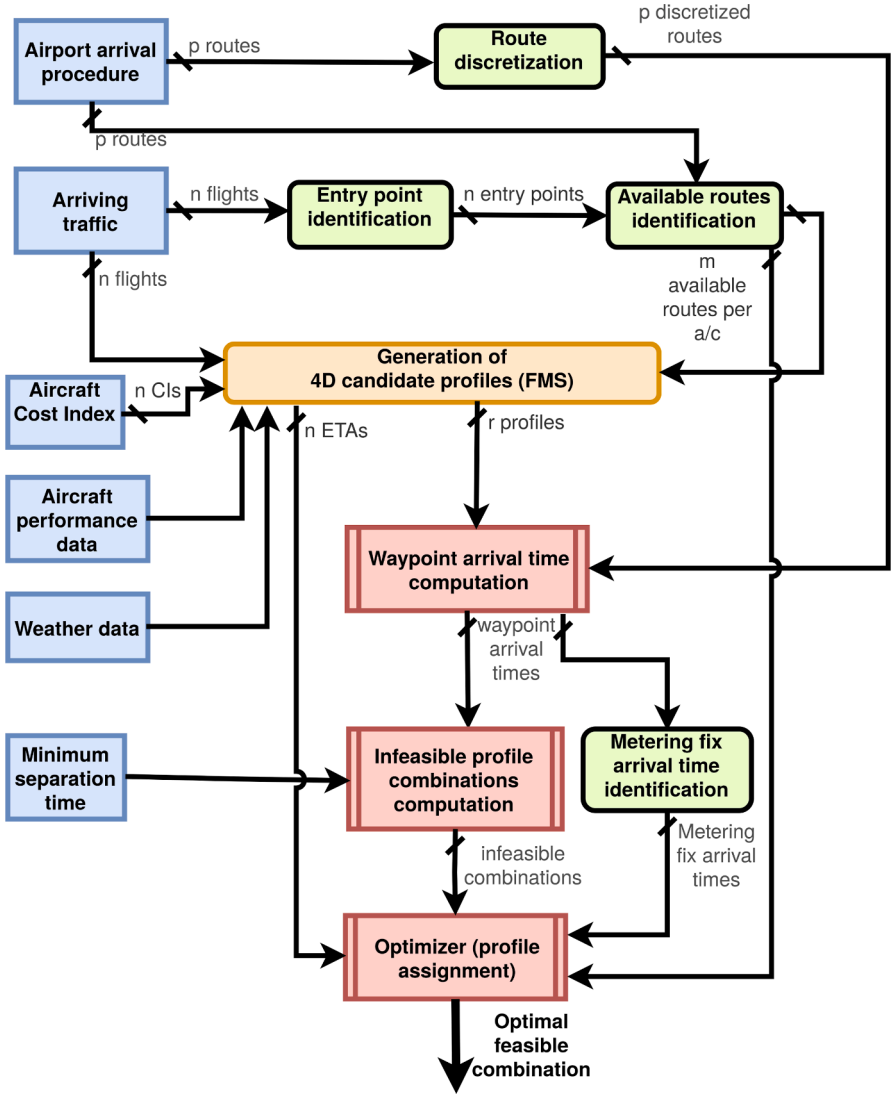


**Fig. 4.** Profile assignment process.

4. The estimated time of arrival (ETA) at the metering fix is also computed by each arriving aircraft FMS according to the cost index set for that particular flight.
5. The arrival times per profile at different waypoints are computed by the FMS, by using all the waypoints generated when discretizing the available routes per aircraft.
6. Infeasible profile combinations are computed on the ground. This involves checking if a minimum time separation is ensured at all waypoints of the procedure between all the aircraft for a given combination of aircraft and profile. Algorithm 1 shows the pseudo-code used to find these infeasible profile combinations by brute force.

Algorithm 1Pseudo-code for finding infeasible profile combinations

```
Define sep. time                                   ▷f is flight, wp waypoint and r route
for f_1 and f_2 in flights do
for wp_1 in waypoints flown by f_1 and f_2 do
  for r_1 in routes flown by f_1 and containing wp_1 do
    for r_2 in routes flown by f_2 and containing wp_1 do
      if abs((wp_1 arrival time of f_1 using r_1) − (wp_1 arrival time of f_2 using r_2)) ⩽ sep.time then
        Save infeasible combination
      else
        Save feasible combination
      end if
    end for
  end for
end for
end for
```

7. The ETA per aircraft, and also the set of possible RTAs at the metering fix (one per profile), together with the infeasible combinations are used as an input to the optimizer. The solution of the aircraft landing problem is the profile-to-aircraft assignments for all aircraft that minimizes a given cost function. The details of this optimization problem are given below.

There are several approaches in the literature focusing on formulating and solving the aircraft landing problem. Regarding its formulation, mixed-integer programming (MIP) is the preferred option by most (if not the totality) of the authors. The problem formulation and the number of variables and constraints involved may vary depending on the airport infrastructure, the runways and routes considered or the number of aircraft to be scheduled. More complex formulations are needed for more complex scenarios, as well as more advanced strategies to solve the problems. In Beasley et al. (2000), the classical MIP formulation for the aircraft landing problem is presented. This formulation sets the basis for some of the future works developed on that topic, such as the job shop formulation presented in Benheikh et al. (2009).

In order to solve the aircraft landing problem, some authors propose to use ant colony algorithms (Beasley et al., 2011), while others just rely on commercial solvers like CPLEX, which solves integer linear problems using either primal or dual variants of the simplex method or the barrier interior point method (Vadlamani and Seyedmohsen, 2014; Samà et al., 2014). In this paper, the aircraft landing problem is modeled as a mixed-integer linear program. The problem formulation is quite simple, as the aircraft profiles are precomputed and are used as the input to the problem. This approach has been chosen mainly because it always outputs optimal solutions. The resulting problem instances corresponding to the real operational scenarios are of relatively small size and are solved in reasonable time using a commercial (CPLEX) solver, as detailed in Section 4.

Let $\mathscr{A}$ be the set containing all aircraft scheduled to land at the airport during a certain period of time. Then, let $\mathscr{P}_a$ be the set containing all possible vertical and speed profiles (a finite number of profiles per available route) that can be flown by a given aircraft $a$ (i.e. one set per aircraft), which are computed by each aircraft FMS. Finally, let $\mathscr{I}$ be the set containing aircraft-profile pairs (e.g. $((a_i, p_k),(a_j,p_r))$) representing the incompatibilities between profiles, meaning that there will be a loss of time separation between aircraft $a_i$ and $a_j$ if aircraft $a_i$ flies profile $p_k$ and aircraft $a_j$ flies profile $p_r$. The required time of arrival at the metering fix $\mathrm{RTA}_{a,p}$ is a known value and corresponds to the arrival time at the metering fix for each profile an aircraft can fly.

Let $x_{a,p}$ be the binary decision variables defined as follows:

$$x_{a,p} = \begin{cases} 1, & \text{if } \textit{aircraft } a \text{ flies profile } p \\ 0, & \text{otherwise} \end{cases} \tag{1}$$

where $a \in \mathscr{A}$ and $p \in \mathscr{P}_a$.

The constraints of the problem are shown in Eqs. (2) and (3). Eq. (2) ensures that if there are incompatibilities between two aircraft flying two profiles, at most one aircraft will be allowed to fly its profile. Otherwise, there would be a loss of separation. On the other hand, Eq. (3) ensures that all aircraft will fly only one profile.

$$x_{a_i,p_k} + x_{a_j,p_r} \leqslant 1, \quad \forall a_i, a_j \in \mathscr{A},\ \forall p_k \in \mathscr{P}_{a_i},\ \forall p_r \in \mathscr{P}_{a_j} \mid ((a_i,p_k),(a_j,p_r)) \in \mathscr{I} \tag{2}$$

$$\sum_{p\in\mathscr{P}_a} x_{a,p} = 1, \quad \forall a \in \mathscr{A} \tag{3}$$

The solution of the aircraft landing problem could be feasible or infeasible depending on the complexity of the scenario. For those feasible scenarios, there may exist many distinct solutions such that all the constraints of the problem are satisfied; namely, each aircraft is assigned one profile compatible with the profiles assigned to all the other aircraft, and an RTA within the feasible time window for that aircraft. In this paper it is considered that the RTA at the metering fix should be as close as possible to the estimated time of arrival ($\mathrm{ETA}_a$) at that fix for each particular flight, assuming that the cost of the (flight) operation is minimized. Thus, the objective function $J$ of the optimization problem formulated in this section is the following:

$$\min J := \sum_{a\in\mathscr{A}}\sum_{p\in\mathscr{P}_a} x_{a,p} \cdot |\mathrm{RTA}_{a,p} - \mathrm{ETA}_a| \tag{4}$$

Aircraft arriving before or later than the ETA are penalized in the same way, so it is assumed that any absolute value of time deviation is detrimental for the arriving aircraft.

Below it is proven that the above-defined problem is NP-hard, which justifies attacking it with an integer program. To show the hardness, it is reduced from Independent Set (IS) – a classical NP-hard problem. An instance of IS is specified by a graph $G$ and an integer $k$; the question is whether $G$ has an independent set of size $k$ (an independent set is a set of vertices no two of which are connected by an edge). See Fig. 5, Left, for an example of this.

Given an instance of IS, an instance of the problem is produced as follows. There will be an aircraft for every vertex in $G$; the aircraft and the vertices are identified with integers from 1 to $n$, where $n$ is the number of the vertices (and hence the aircraft). Every aircraft $v$ will have two profiles: a *fast* profile $f_v$ and a *slow* profile $s_v$. If $v$ follows the fast profile, then the aircraft arrives at time $v$; if $v$ follows $s_v$, then it arrives at time $n+v$ (Fig. 5, Right). When creating the profiles, the following rules are adhered: if vertices $u, v$ are connected by an edge in $G$, then using the fast profiles $f_u, f_v$ together will lead to separation loss between aircraft $u$ and $v$. On the contrary, any slow profile does not conflict with any other profile (slow or fast), i.e., using any slow profile is possible irrespective of what profiles are chosen for all other aircraft.

Finally, the ETA of aircraft $v$ is set to $v$. That is, if all aircraft follow fast profiles, the objective function is 0. More generally, the objective function is equal to $(n-k)n$ if and only if exactly $k$ aircraft follow fast profiles (because $n$ is added to the objective function for every aircraft following slow profile). But the set of aircraft following fast profiles corresponds to an independent set in $G$. Hence $G$ has an independent set of size $k$ if and only if the objective function in our problem is at most $(n-k)n$.

Since the optimization problem is NP-hard, it is non-convex (a convex problem could be solved in polynomial time).

### 2.4. Trajectory optimization problem

In this paper, several trajectories (i.e. profiles) are generated for each aircraft arriving at the destination airport; they are computed for different times of arrival within the available metering fix time window and for each possible alternative route. In this subsection the underlying computations and theory behind steps 3 and 4 of Section 2.3 are explained (corresponding to the yellow box of Fig. 4 - *Generation of 4D candidate profiles (FMS)*).

Given a known route, and consequently a fixed distance to go, the optimization of the vertical profile (altitude and speed) can be formulated as an optimal control problem, which aims at computing the control time history of a system, here the aircraft, such that a cost function is minimized while satisfying some dynamic and operational constraints. Several approaches can be found in the literature addressing this problem, like the ones found in Prats et al. (2017), Dalmau et al. (2016), which focused on the development of advanced concepts and technologies in order to satisfy RTAs with high accuracy. In this work, the solution chosen is the semi-analytic trajectory optimizer proposed in Park et al. (2017), which proved to be very robust and fast.

#### 2.4.1. Generic optimal control problem

A generic single-phase optimal control problem, over a continuous time horizon $[t_0, t_f]$ is defined as follows:

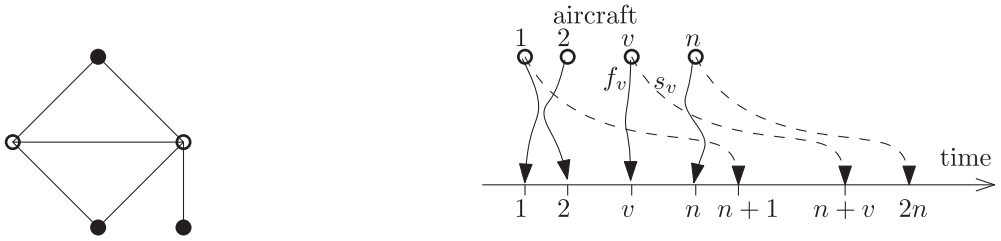


**Fig. 5.** Left: A graph $G$ with 5 vertices, and an independent set (black) with 3 vertices. Right: Each of the $n$ aircraft has two profiles; the vertices 1 and 2 are connected by an edge in $G$ and hence their fast profiles cannot be used simultaneously (a loss of separation will occur).

$$\begin{aligned} \min_{u(t)} \quad & J_a := \phi\big(x(t_f)\big) + \int_{t_0}^{t_f} L(x(t), u(t), p)\mathrm{d}t \\ \text{s.t} \quad & x(t_0) = x_0 \\ & x(t_f) = x_f \\ & \dot{x}(t) = f(x(t), u(t), p) \\ & h(x(t), u(t), p) \leqslant \varnothing 0 \end{aligned} \tag{5}$$

where $x \in \mathbb{R}^{n_x}$ is the state vector, with fixed initial conditions $x_0$ and fixed final conditions $x_f$; $u \in \mathbb{R}^{n_u}$ is the control vector; and the vector $p \in \mathbb{R}^{n_p}$ includes all the time-independent parameters of the model; $L : \mathbb{R}^{n_x} \times \mathbb{R}^{n_u} \times \mathbb{R}^{n_p} \to \mathbb{R}$ and $\phi : \mathbb{R}^{n_x} \to \mathbb{R}$ are the so called Lagrange and Mayer terms of the cost function, respectively. The dynamics of the state vector are expressed by a set of non-linear equations $f : \mathbb{R}^{n_x} \times \mathbb{R}^{n_u} \times \mathbb{R}^{n_p} \to \mathbb{R}^{n_x}$; while $h : \mathbb{R}^{n_x} \times \mathbb{R}^{n_u} \times \mathbb{R}^{n_p} \to \mathbb{R}^{n_h}$ represent applicable path constraints. Note that if the time interval is not fixed, $t_f$ becomes a decision variable itself.

The Hamiltonian of the optimal control problem (5) is:

$$H = L + \boldsymbol{\lambda}^T f + \boldsymbol{\mu}^T h, \tag{6}$$

where $\boldsymbol{\lambda}$ and $\boldsymbol{\mu}$ are vectors of Lagrange multipliers. The set of necessary conditions for $J_a$ to be stationary optimum and more details about optimal control theory can be found in Bryson and Ho (1975).

#### 2.4.2. Optimal control problem for aircraft descents

In this paper, the state vector is composed of the true airspeed (TAS), the altitude of the aircraft, and the distance to go ($x = [v, h, s]$). The dynamics of $x$ are expressed a set of ordinary differential equations (ODE), assuming a point-mass representation of the aircraft reduced to a the so called "gamma-command" model, where vertical equilibrium is assumed.

In order to obtain environmentally friendly trajectories, idle thrust is imposed and speed brakes use is not allowed throughout the descent. Therefore, the aerodynamic flight path angle is the only control variable steering this dynamical system ($u = [\gamma]$).

The cross and vertical components of the wind are neglected in the dynamics of $x$, only considering the longitudinal component of the wind $w$ projected in the same direction of the flight. Furthermore, the aerodynamic flight path angle is assumed to be small (i.e., $\sin\gamma \simeq \gamma$ and $\cos\gamma \simeq 1$) and international standard atmosphere (ISA) conditions are assumed.

Taking all previous considerations into account, the dynamics of $x$ are given by:

$$f = \begin{bmatrix} \dot{v} \\ \dot{h} \\ \dot{s} \end{bmatrix} = \begin{bmatrix} \dfrac{T_{idle} - D}{m} - g\gamma \\ v\gamma \\ v + w \end{bmatrix}, \tag{7}$$

where $T_{idle} : \mathbb{R}^{n_x} \to \mathbb{R}$ is the idle thrust; $D : \mathbb{R}^{n_x \times n_u} \to \mathbb{R}$ is the aerodynamic drag; $g$ is the gravity acceleration and $m$ is the mass of the aircraft, of which is assumed to be constant because the fuel consumption during an idle descent is a very small fraction of the total mass (Clarke et al., 2004).

In this work, the longitudinal component of the wind is modelled by a smoothing spline (de Boor, 1972), $w : \mathbb{R} \to \mathbb{R}$, such that:

$$w(h) = \sum_{i=1}^{n_c} c_i B_i(h), \tag{8}$$

where $B_i, i = 1, \ldots, n_c$ are the B-spline basis functions and $c = [c_1, \ldots, c_{n_c}]$ are the control points of the smoothing spline.

It should be noted that the longitudinal wind has been modelled as a function of the altitude only, as done in similar works (de Jong et al., 2014). The control points of the spline approximating the longitudinal wind profile are obtained by fitting historical weather data.

In this paper, the trajectory considered covers the latter part of the cruise phase and all the descent down to the metering fix where the RTA will be assigned. It is assumed that the original cruise speed is maintained (and therefore, not subject to optimization). Yet, the fuel consumption in cruise is considered in the objective function, since the location of the top of descent (TOD) is indeed subject to optimization. This problem can be modeled as a single-phase optimal control problem that minimizes a compound function that takes into account both fuel and time costs (Park et al., 2017), relating them with the Cost Index (*CI*) ratio. Expressing the cost function in Lagrange form:

$$J_a = \int_{t_0}^{t_f} -\left(\frac{f + \mathrm{CI}}{v_{cr}}\right)(v + w) + f_{idle} + \mathrm{CI}\; dt \tag{9}$$

where $v_{cr}$ is the cruise speed (which is assumed to be constant), $f : \mathbb{R}^{n_x \times n_u} \to \mathbb{R}$ is the cruise fuel flow (which is assumed to be constant, since the cruise altitude and speed are also constant) and $f_{idle} : \mathbb{R}^{n_x} \to \mathbb{R}$ is the idle fuel flow in the descent (which depends on the speed and altitude).

In addition to the dynamic constraints $f$, the following path constraints are enforced to ensure that the aircraft airspeed remains within operational limits; that the aircraft is not climbing and that a given minimum descent gradient is not exceeded:

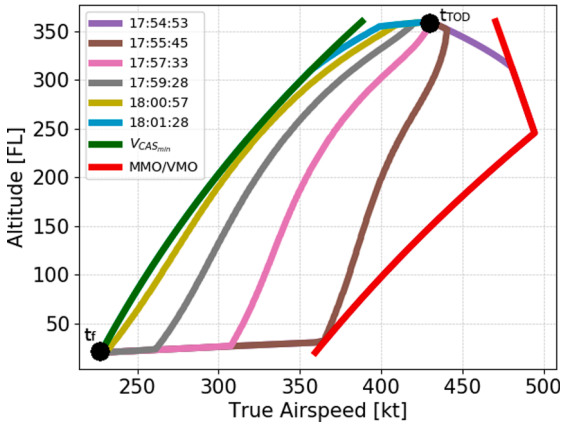


**Fig. 6.** Example of optimal speed profiles for an Airbus A320 Neo and several required times of arrival in ISA and no wind conditions.

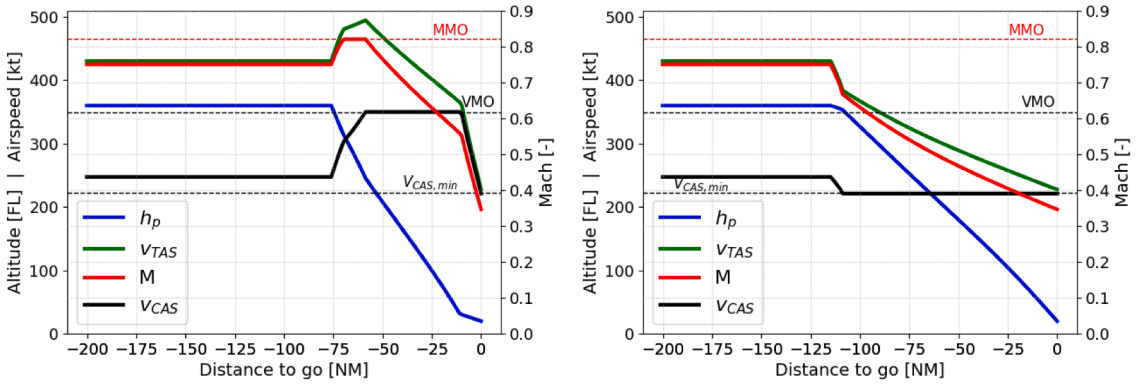


(a) Earliest trajectory (RTA = 17:46:17)

(b) Latest trajectory (RTA = 18:01:28)

**Fig. 7.** Illustrative earliest and latest trajectories for an A320 Neo in ISA and no wind conditions.

$$h = \begin{bmatrix} v_{CAS,min} - v_{CAS} \\ v_{CAS} - \text{VMO} \\ M - \text{MMO} \\ \gamma \\ \gamma_{min} - \gamma \end{bmatrix} \leqslant \begin{bmatrix} 0 \\ 0 \\ 0 \\ 0 \\ 0 \end{bmatrix} \tag{10}$$

where $v_{CAS} : \mathbb{R}^{n_x} \to \mathbb{R}$ is the calibrated airspeed (CAS) and $M : \mathbb{R}^{n_x} \to \mathbb{R}$ is the Mach number, both functions of the state vector; $v_{CAS,min}$ and VMO are the minimum and maximum operative CAS, respectively; MMO is maximum operative Mach; and $\gamma_{min}$ is the minimum descent gradient (recall it is a negative value).

Different alternatives can be used to model the functions that depend on aircraft performance ($T_{idle}, D, f, f_{idle}$) and their respective parameters, such as the EUROCONTROL's base of aircraft data (BADA) (Poles et al., 2010).

In the formulation presented herein, there is only one control variable $\gamma$, which appears linearly in the equations describing the dynamics of the system as well as in the cost function. Consequently, the Hamiltonian of the system (6) is also linear with respect to this control, leading to a singular optimal control problem which can be solved semi-analytically from the implicit formulation of optimal singular arcs (Park et al., 2017).

Since the initial and final states of the trajectory are fixed, the optimal trajectory will be of a "bang-singular-bang" type. These solutions consist of three arcs: one non-singular arc with the control variable at its maximum or minimum value to go from $x_0$ to the singular arc; a singular arc where the optimal control is given as a function of the states vector; and a final non-singular arc to go from the singular arc to the final state $x_f$. This model, however, has some limitations. It can only be used to optimize the descent or climb vertical profiles, while the lateral profile is not optimized. Furthermore, RTAs can only be achieved by brute force, iterating over the several cost indexes. However, for the purposes of this work, it is a very good choice given its robustness and speed. As the trajectory optimization technique used is not based on a non-linear solver, there are no convergence problems and a solution is always found. Furthermore, the computational time spent to generate a single trajectory was less than 5 s in all cases. The analytical expression of the

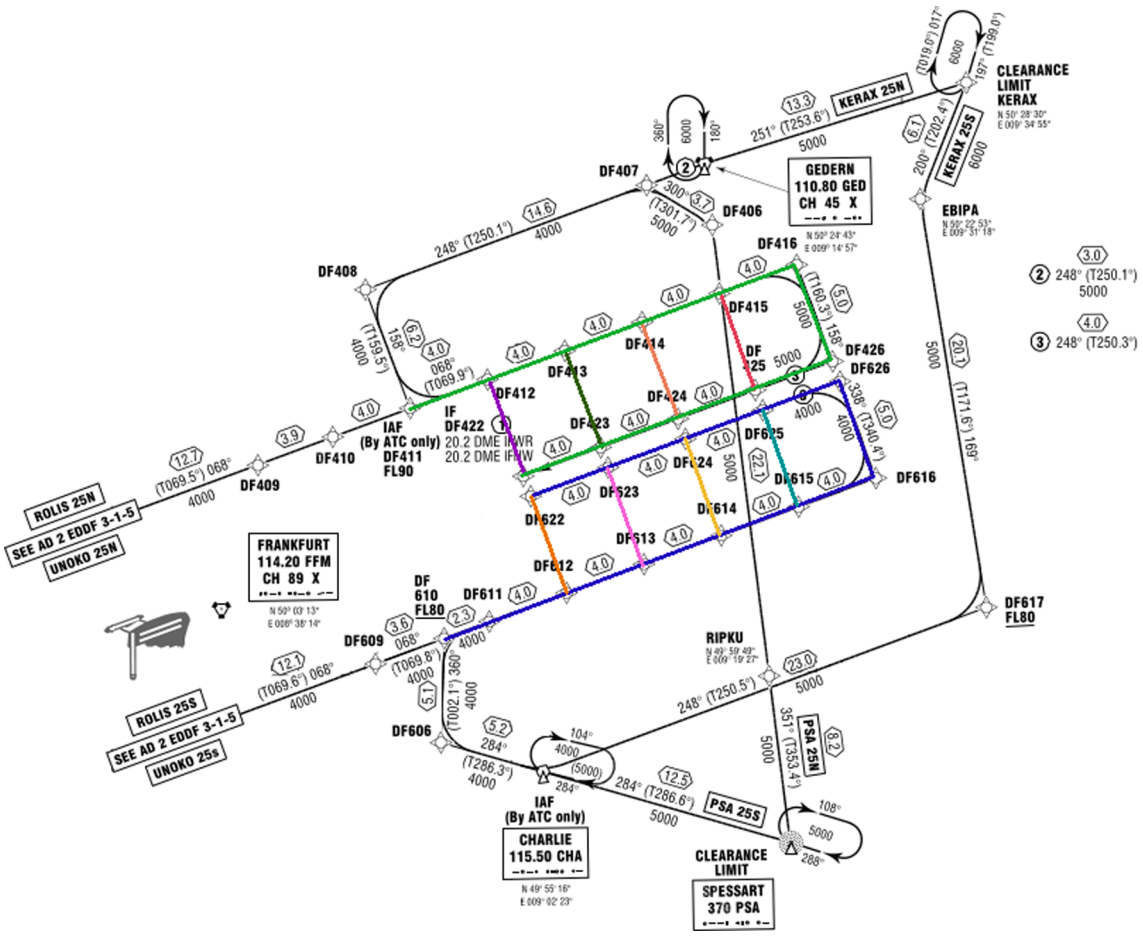


**Fig. 8.** Frankfurt am Main Airport (EDDF) GPS/FMS RNAV 25L/C/R Tromboning (source: German AIP).

optimal control in the singular arc for the above model, and the steps to generate an optimal trajectory semi-analytically can be found in Park et al. (2017).

As an example, Fig. 6 shows several optimal speed profiles for an Airbus A320 Neo and for several CIs (i.e. RTAs), in international standard atmospheric (ISA) conditions and no wind. A distance to go of 378 NM, a cruise true airspeed of 430 kt and a cruise altitude at FL360 were used as initial conditions for the generation of these illustrative trajectories. The initial time ($t_0$) was set at 17:01:31 and the final state was defined assuming a distance to go of 0 NM, a final altitude of 2,000 ft and a final airspeed equal to the green dot speed[3].

The "bang-singular-bang" behavior can be observed in these speed profiles, with an arc from the time when the descent starts ($t_{TOD}$ in Fig. 6)) to the singular arc and a final arc from the singular arc to the final time at the metering fix ($t_f$ in Fig. 6). It can be observed how the optimal speed profiles lie in between the boundaries delimited by $v_{CAS,min}$ and MMO/VMO, as enforced by Eq. (10). Also note that since these maximum and minimum speeds are given in terms of CAS and Mach, the corresponding TAS changes with altitude. The earlier the RTA, the closer the speed profile is to the MMO/VMO bound and, on the other hand, the later the RTA the closer the speed profile is to the $V_{CAS_{min}}$ line; therefore, the speed profiles corresponding to the earliest and latest trajectories (purple and cyan lines respectively) try to match as soon as possible the MMO/VMO and $v_{CAS,min}$ speed profiles respectively.

Fig. 7 shows the evolution of the aircraft altitude and speed, as a function of the remaining distance to the metering fix, for the earliest (17:46:17) and latest (18:01:28) trajectories corresponding to the illustrative flight presented before. Note that the y-left axis is used to represent both altitude and airspeed. As commented before, in this study the cruise speed is kept constant to the originally planned speed, optimizing only the descent trajectory. In Fig. 7(a) it is observed how the aircraft accelerates to the MMO right after the TOD. This descent at constant Mach implies an increase of the CAS and, when reaching the VMO, the descent continues at this maximum speed. Few nautical miles before the metering fix a quick deceleration is observed in order to fulfill the speed constraint at

[3] For the Airbus A320 Neo, the green dot speed is the minimum operating speed in managed mode and clean configuration, being approximately the best lift-to-drag ratio speed.

this fix. Fig. 7(b), in turn, shows the latest trajectory, which slows down to $v_{CAS,min}$ right after the TOD.

## 3. Experimental setup

This section presents the experimental setup used to illustrate the concept of operations and methodology proposed in this paper, where all incoming aircraft are assigned the shortest possible route, allowing them to attain an RTA at the metering fix as close as possible to their ETA and without incurring a time separation loss with the surrounding traffic. Frankfurt's airport trombone procedure has been chosen for this study. A hypothetical extended TMA (E-TMA) of 250 NM of radius is defined around the airport. In addition, the current STAR procedures are extended with a straight line from the first waypoint of each STAR to the aircraft entry points to the E-TMA. As soon as they enter the E-TMA, aircraft are assigned an RTA and a route (after pre-negotiation with the ATCO). Then, they are assumed to fly the extended STAR, after which they start the trombone procedure to follow the assigned route.

### 3.1. Frankfurt arrival and approach procedures

Frankfurt airport is by far the busiest airport in Germany as well as the fourth busiest in Europe. This airport is provided with four runways, of which three are disposed parallel in east–west direction and one in north–south direction. During normal operation, the two outer parallel runways (07L/25R and 07R/25L) are used for arrivals and the north–south runway (18–36) and the central parallel runway (07C/25C) for departures. In this paper, the GPS/FMS RNAV 25L/C/R transition to final approach (i.e. west configuration) is used, which is a trombone procedure, assuming aircraft could land either in 25L (i.e. north) or 25R (i.e. south) runways. Fig. 8 shows this procedure. Note that the altitude in the last segment of the trombone procedure (waypoints from DF426 to DF422 and waypoints from DF626 to DF622 for north and south arrivals respectively) is different, being 4,000 ft for south arrivals and 5,000 ft for north arrivals. Therefore, in the final segment aircraft are separated vertically by 1,000 ft.

Apart from the tromboning, standard arrival route (STAR) procedures are also used. There are 7 STAR entry points in Frankfurt airport. PSA, ROLIS, UNOKO and KERAX are shown in Fig. 8. EMPAX, ASPAT and PETIX STARs all converge in PSA, from where they continue the PSA STAR. In addition, each entry point allows the aircraft to fly the arrival procedure to both the north or the south runway (e.g. KERAX 25S and PSA25S lead to runway 25L; and KERAX 25 N and PSA25N lead to runway 25R). The tromboning common part for all entry points starts at waypoint DF411 for the north runway (colored in green in Fig. 8) and at DF610 for the south runway (colored in blue in Fig. 8). From these points on, the ATCO could potentially give a shortcut at any of the regularly spaced waypoints, depending on the volume of traffic. Thus, for each entry point there are only 5 possible routes, as it is only possible to assign 5 shortcuts in the trombone. For the north runway arrivals, the shortcuts are given in waypoints from DF412 to DF416 (both included), and for the south runway arrivals in waypoints from DF612 to DF616 (both included). The tromboning ends at the intermediate fix (IF) of the approach, which is the waypoint DF422 for the north and DF622 for the south runways, respectively.

Table 1 shows all potential tromboning routes for north and south runway arrivals, identified with different colors as in Fig. 8. Route numbers from 01 to 05 correspond to arrivals to the north runway while route numbers from 06 to 10 correspond to arrivals to the south runway. The higher the route number the shortest the route (for north and south respectively). In this table, the distance for each tromboning route is also given. For instance, for route 08, corresponding to the south case, a shortcut is given at DF614 towards DF624, skipping the waypoints from DF615 to DF625 and reducing by 16 NM the total distance flown. Finally, the metering fix for each runway has been set to the respective intermediate fixes (DF422 and DF622).

### 3.2. Input data

The assessment has been performed by using flight traffic data from August 10th, 2017. These data have been obtained from EUROCONTROL's data demand repository (DDR2) (Eurocontrol, 2017), which contains historical trajectory data (M3 format). In that day, there were 731 flights (divided into 52 aircraft types) arriving at Frankfurt airport; the demand per hour, in Coordinated Universal Time (UTC), is shown in Fig. 9.

In this work, three time periods of the day of study are selected to validate the proposed algorithm, which represent three different

**Table 1**
Potential routes for Frankfurt trombone procedure (North and South cases).

| ID | Waypoint sequence | Distance [NM] |
|---|---|---|
| 01 | DF411-...-DF416-DF426-...-DF422 | 41 |
| 02 | DF411-...-DF415-DF425-...-DF422 | 33 |
| 03 | DF411-...-DF414-DF424-...-DF422 | 25 |
| 04 | DF411-...-DF413-DF423-DF422 | 17 |
| 05 | DF411-DF412-DF422 | 9 |
| 06 | DF610-...-DF616-DF626-...-DF622 | 43.3 |
| 07 | DF610-...-DF615-DF625-...-DF622 | 35.3 |
| 08 | DF610-...-DF614-DF624-...-DF622 | 27.3 |
| 09 | DF610-...-DF613-DF623-DF622 | 19.3 |
| 10 | DF610-...-DF612-DF622 | 11.3 |

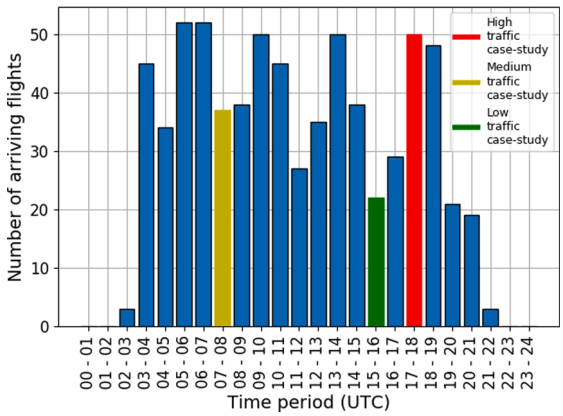


**Fig. 9.** Frankfurt airport demand per hour on August 10th, 2017. The 3 case-studies are highlighted.

traffic situations (they are highlighted in different colors in Fig. 9). They correspond to the three baseline case-studies:

- High traffic case-study (red): from 17 to 18 UTC
- Medium traffic case-study (yellow): from 07 to 08 UTC
- Low traffic case-study (green): from 15 to 16 UTC

For the optimization of CDO trajectories, the upper bounds on the speed limits (VMO and MMO), which are aircraft dependent, are obtained from the BADA v4.1 aircraft performance files; the minimum speeds $v_{CAS,min}$ correspond to the green dot speed; and the maximum descent gradient ($\gamma_{min}$) is set to $-7°$.

The initial state of the aircraft, consisting of the cruise altitude, cruise speed and distance to go, is obtained directly from DDR2 in the position where the aircraft enter the E-TMA. The terminal constraints defined in Section 2.4.2 are the following: the final speed $v_{RTA}$ corresponds to the green dot speed, the altitude $h_{RTA}$ is equal to 2,000 feet and the distance to go $s_{RTA}$ is equal to 0 NM.

The weather data used to generate the longitudinal wind profile as a function of the altitude are obtained from gridded binary (GRIB) formatted files provided by the global forecast system (GFS) of the National Oceanic and Atmospheric Administration (NOAA). For each arriving flight, the GRIB file corresponding to its entry point at the E-TMA time is used.

### 3.3. Separation considerations

A separation between aircraft has to be ensured in order to maintain the safety of the operation. The separation will be defined by taking into account the wake turbulence categorization proposed by ICAO (SKYbrary, 2020), which classifies aircraft into three categories depending on their maximum take-off mass. In this work, the minimum time separation between aircraft that ICAO proposes according to that categorization (ICAO, 2016) will be used: 180 s of time separation will be considered for light aircraft following medium or heavy aircraft, while 120 s will be considered otherwise. During the day chosen for the experiment, there were 184 heavy aircraft, 544 medium aircraft and 2 light aircraft (17 heavy, 52 medium and 2 light different aircraft types among all the arriving traffic). The distribution of aircraft in the case-studies chosen was the following:

- High traffic case-study: 5 heavy and 45 medium aircraft (4 heavy and 9 medium different aircraft types)
- Medium traffic case-study: 9 heavy and 28 medium aircraft (7 heavy and 9 medium different aircraft types)
- Low traffic case-study: 6 heavy and 16 medium aircraft (5 heavy and 10 medium different aircraft types)

As it has been mentioned in Section 3.1, a separation of 1,000ft between north and south arrivals is ensured in the final segment of the tromboning. However, in this work, neutral CDOs are assumed, which means that this vertical separation is not necessarily ensured. Therefore, it would be considered that the runways are not independent and that a lateral separation should also be ensured between north and south arrivals in the final segment. This means that, for instance, it would not be possible that two aircraft are at the same time at waypoints DF424 and DF624 (Fig. 8).

### 3.4. Profiles computation

All routes that can be found in the Frankfurt airport arrival and approach charts are discretized in 5-NM-length segments. Then, 10 profiles are generated per available route an aircraft can fly, with RTAs equally spaced in time in the available time window at the metering fix. This means that if the time window at the metering fix for a given aircraft flying a given route is, for instance, equal to nine minutes, there will be one profile per minute (both the earliest and latest arrival times to the metering fix are included). This is illustrated in Fig. 10, where $p$ stands for profile (e.g. $p1$ is profile 1). $RTA_E$ and $RTA_L$ are the earliest and latest times of arrival at the

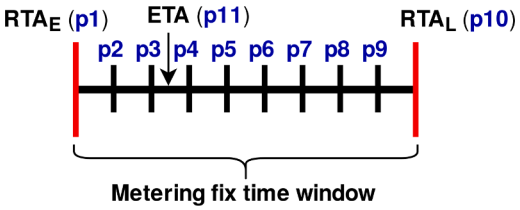


**Fig. 10.** Time window and candidate profiles for a given route.

metering fix for a given route respectively.

It is worth noting that this time window (defined as the difference between the earliest and latest arrival times to the metering fix) is computed per available route. Therefore, the final time window or "absolute" time window for each aircraft used in the scheduling algorithm will be given as the difference between the earliest time of arrival for the shortest route and the latest time of arrival for the longest route.

Finally, an extra profile is generated and added to the set of profiles, which corresponds to the desired trajectory by the airline that gives the estimated time of arrival (ETA) at the metering fix. In this paper, the shortest route per aircraft is considered to compute this ETA, along with the speed (and time) profiles extracted from the DDR2 data.

### 3.5. Model enhancements

Apart from performing the profile assignment for the three case-studies defined in Section 3.2, which will be referred in the remainder of the paper as *baseline* case-studies, six additional enhancements are added to the scenario analyzed in this paper. In case of infeasible scenarios, in which not all aircraft can be scheduled, these enhancements could help to improve the results.

- **Additional shortcuts**: in the current Frankfurt trombone procedure there are 10 available shortcuts per STAR entry point, 5 for the north and 5 for the south (more details in Section 3.1). The number of shortcuts could also be modified in order to add more possible routes for the incoming aircraft. In this case, three waypoints are added between waypoints DF407 and DF408, which suppose three new shortcuts, as shown in Fig. 11.
- **Entry time**: the arrival time to the E-TMA is manually modified for all incoming aircraft, seeking to improve the output of the aircraft landing problem (i.e. to maximise the number of neutral CDOs while ensuring a safe separation between aircraft). Two additional case-studies are considered, one with a maximum variation of ±2 min in the entry time and another one with a maximum variation of ±5 min. For instance, in the ±2 min case, if an aircraft was expected to arrive at 10:00 at the E-TMA, it is assumed that it could also arrive at 9:58 and 10:02. In a real situation, this change in the entry time could be achieved during the en-route phase. As shown in previous works, these modifications in the entry time are feasible. From the results obtained in Delgado and Prats (2012), it can be concluded that, for typical cost indexes between 30 kg/min and 100 kg/min, aircraft can gain/lose between 1.2 s/NM and 4 s/NM. Therefore, assuming a cruise length of between 75 NM and 250 NM aircraft would be able to arrive 5 min earlier or later to the E-TMA entry point. These values depend on several factors, like the aircraft type or the cruise flight level. Furthermore, the wind can also affect the amount of time that can be gained/lost during cruise (Delgado and Prats, 2013).
- **Fairness in the delay assignment**: the cost function used in the aircraft landing problem (Eq. (9)) does not consider any equity between flights when assigning delay. Therefore, a new cost function has been defined in order to assign delays moderately across

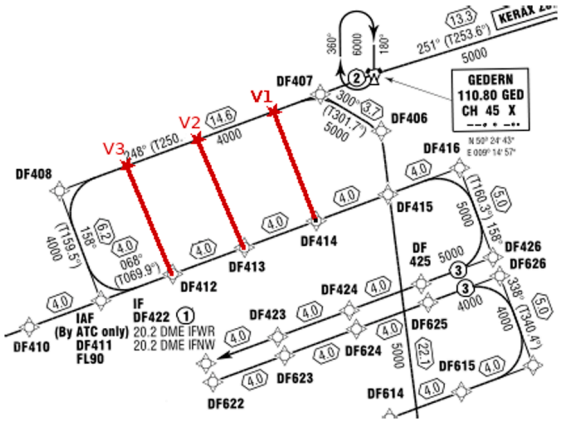


**Fig. 11.** Three new shortcuts in Frankfurt am Main Airport (EDDF) GPS/FMS RNAV 25L/C/R trombone procedure (source: German AIP).

all flights, instead of unevenly to one particular flight (Bertsimas and Patterson, 1998). The total delay is raised to a given coefficient $(1+\epsilon)$ (with $\epsilon$ slightly greater than 0) as follows:

$$\min J := \sum_{a\in\mathcal{A}}\sum_{p\in\mathcal{P}_a} x_{a,p}\cdot\left(\left|\mathrm{RTA}_{a,p}-\mathrm{ETA}_a\right|\right)^{(1+\epsilon)} \tag{11}$$

This is just a preliminary approach toward the consideration of fairness in the delay assignment; in future work it is planned to explore more fairness strategies.

- **Time separation**: in the baseline case-studies RTAs are assumed to be met with a 100% of accuracy. However, this is not the case in actual operations, as perturbations during flight may introduce errors in meeting the RTA. However, it has been shown that RTAs can be achieved with errors lower than 10 s at the final approach point (Prats et al., 2017), while a good RTA accuracy can be maintained too in presence of significant wind prediction errors (Dalmau et al., 2016). Further guidance improvements were proposed in Dalmau et al. (2019), showing even better results in terms of RTA accuracy for neutral trajectories (using only energy modulation). All these works endorse our assumption that RTAs can be achieved with high levels of accuracy, thus enabling robust neutral CDOs. Still, inaccuracies will be always present, so based on the aforementioned results, another case will be analyzed, in which the minimum time separation between the arriving aircraft is increased by 20 s. This corresponds to the worst case scenario if an accuracy of 10 s in the RTA is assumed: if considering two aircraft with their corresponding RTAs separated by 120 s, the worst situation would be the one in which the leading aircraft is arriving at the metering fix 10 s later than its RTA and the trailing aircraft arrives 10 s earlier.
- **Independent runways**: independent runways are assumed in this enhancement, which means that during the final segment of the tromboning a vertical separation is supposed to be maintained between the north and south arrivals. As a result, it is no longer necessary to maintain a lateral separation between traffic arriving to different runways in the final segment of the tromboning. This assumption is endorsed by Fricke et al. (2015), in which it is described that, for any given flight, a *vertical CDO corridor* can be defined, in which all the flyable CDOs are contained. However, not all these CDOs would be optimal from an efficiency point of view. Still, the definition of these corridors would be useful to apply the methodology described in this paper for a procedure with independent runways. By applying altitude restrictions in the corridors it would be possible to force the aircraft to fly those trajectories that ensure a vertical separation in the final segment of the tromboning. This may lead to fly sub-optimal CDOs, but it would keep the safety of the operation.

## 4. Results

This section presents the results obtained after simulating the scenario and case-studies described in Section 3. Section 4.1 presents an analysis of the time window for all cases. Then, Section 4.2 analyzes the results obtained for the baseline case-studies, while more details are given in Section 4.3. It is shown that not all aircraft can be scheduled in all three baseline case-studies, mainly due to high traffic density in the medium and high traffic cases and the fact that only neutral CDOs are assumed. Better results are presented in Section 4.4, showing how by changing some parameters (Section 3.5) it is possible to increase the number of neutral CDOs with a safe separation in the medium and high traffic cases. Regarding computational times, the set of profiles was generated in around 5 min per aircraft. Then, the incompatible profiles were found in 10 to 30 min (depending on the volume of traffic) and finally, the optimizer (the mixed integer linear program) took between 1 and 5 min (depending on the volume of traffic) to find the optimal feasible profile combination. All computations were made in a laptop computer running Ubuntu 18.04 LTS, with 16 GB of RAM memory and an Intel (TM) Core(R) i7-7500U @ 2.70 GHz processor. While these computational times might seem high, they are enough to generate the flight arriving sequence. However, in this case, aircraft might need to establish the communication with the ATC before entering the E-TMA, so that the RTA and the route are assigned before the optimal top of descent.

### 4.1. Time windows analysis

As detailed in Section 3.4, 11 profiles are computed per available route an aircraft can potentially fly, being the “absolute” time window the difference between the earliest time of arrival for the shortest route and the latest time of arrival for the longest route. The time window is affected by the aircraft model, and by the entry point, which will determine the potential routes an aircraft could fly.

Fig. 12 shows the time window value distribution for the three traffic case-studies. As it can be observed, the median value for the all cases is very similar, around 650 s (≈10 min). Maximum values of up to 1000 s (≈16 min) are observed in the high traffic case-study, while the minimum value, found in the medium traffic case, is 200 s (≈3 min).

For illustrative purposes, Fig. 13 shows the time windows at the metering fix for all available routes of an Airbus A320 Neo flying the EMPAX arrival procedure. The time in the x axis corresponds to the time flown since the E-TMA entry point while the aircraft is still in cruise until the metering fix. For every route, time windows are about 6 to 7 min, being the total time window in the metering fix (i.e. the difference between the earliest and latest times of arrival considering all routes) around 15 min. It can be observed how several

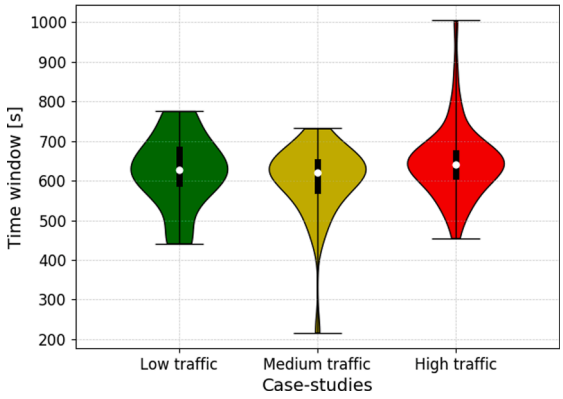


**Fig. 12.** Time windows for the baseline case of the 3 traffic case-studies.

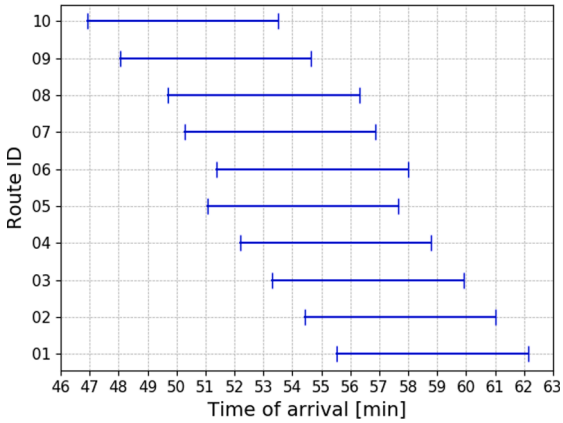


**Fig. 13.** Time windows for the available routes of an A320 Neo flying the EMPAX arrival procedure.

routes could be chosen to attain the same RTA, although in some cases this would mean not flying with the optimum speed profile.

The computation of the vertical and speed profiles is of high importance for the work presented in this paper, as it allows to know the earliest and latest times of arrival to the metering fix and, therefore, the feasible time window for each distance to go corresponding to a trombone shortcut. Fig. 7 in Section 2.4.2 showed the earliest and the latest trajectories for the same A320 Neo used to generate the time windows of Fig. 13, which flew the Frankfurt EMPAX arrival procedure. The earliest case corresponds to route 10 of the arrival procedure and the latest case to route 01 (Table 1).

### *4.2. Profile assignment results*

Table 2 shows the percentage of aircraft successfully scheduled for the three traffic case-studies. As it can be observed, only for the low traffic case-study all aircraft can be scheduled. While the number of aircraft in the low traffic case-study is 22, in the time periods corresponding to the medium and high traffic case-studies (7–8 UTC and 17–18 UTC respectively) there were 37 and 50 aircraft arriving at Frankfurt airport.

As the traffic density increases, it becomes more difficult to schedule all aircraft with the current trombone procedure and entry times. The number of aircraft merging in the several waypoints of the procedure increases, and time separation cannot be ensured

**Table 2**
Percentage of aircraft scheduled per case-study.

| Case-study | Number of aircraft (in 1 h) | % aircraft scheduled |
|---|---|---|
| Low traffic | 22 | 100% |
| Medium traffic | 37 | 84% |
| High traffic | 50 | 68% |

throughout the descent for any combination of route and RTA at the metering fix.

At this point, it is worth recalling that all the trajectories being considered in this work are neutral CDOs with idle thrust and no speed-brakes usage, so the time windows in the metering fix are smaller than those that can be achieved with conventional procedures or powered CDOs (where thrust and speed-brakes are allowed). Therefore, there is not much flexibility regarding the arrival time in the metering fix, which makes the aircraft scheduling process more challenging. In a real situation, all traffic that cannot be accommodated with neutral CDOs would eventually be sequenced by giving RTAs requiring thrust/speedbrakes or even level-offs (so, *breaking* the CDO). The optimal solution for these case-studies where not all aircraft can fly a neutral CDO is an interesting research problem that will be assessed in future work. The purpose of this paper is to show that the proposed concept of operations already allows to fly neutral CDOs to a very significant percentage of the incoming traffic.

Finally, only 11 profiles per aircraft and route are considered in this work. Perhaps a finer discretization could help to potentially find more feasible profiles.

Fig. 14 shows the delay distribution (i.e the difference between the RTA and ETA) for the three baseline case-studies, by taking into consideration only those aircraft that were successfully scheduled. The low traffic case-study shows relatively low delay values, where most of the aircraft scheduled are landing close to their ETA. On the other hand, the medium and high traffic case-studies show a different behavior, where a large number of aircraft is assigned a high delay in order to sequence all traffic. Still, in both cases the maximum delay remains below 650 s (≈11 min). This is understandable as the value of maximum delay that could be achieved is strictly related to the value of the time window: it is impossible for an aircraft to have a higher delay than its time window width. Both the medium and high traffic case-studies show a similar distribution (with a slightly higher dispersion in the high traffic case). However, although the percentage of aircraft scheduled is higher in the medium case, it represents almost the same number of aircraft than in the high case (31 and 34 aircraft respectively). This leads to the conclusion that similar results would be obtained if the traffic density kept increasing: the distribution would be similar but the percentage of aircraft scheduled would decrease.

Fig. 15 shows the extra distance flown for the three baseline case-studies and for the two versions of the cost function: with and without considering fairness in the delay assignment. When possible, the scheduling algorithm tries to assign the shortest route to the aircraft. This is well illustrated in the low traffic case, where 11 aircraft (half of the aircraft sample during that hour) are assigned the shortest possible route. In the medium traffic case more shortcuts are used in order to maintain separation, and the extra distance flown increases. This is more obvious in the high traffic case, where only one third of aircraft are assigned the shortest possible route, while the rest are assigned longer shortcuts.

### 4.3. *Detailed results for the baseline case-studies*

Table 3 shows all aircraft arriving in Frankfurt airport for the low traffic case-study, the totality of which were successfully scheduled with the solution proposed in this work. The DDR2 flight id, the STAR entry point and the ETA for the incoming traffic are given. Furthermore, the route and RTA assigned to each aircraft are shown (i.e. profile), as well as the corresponding delay when flying that profile.

As it can be observed in Table 3, the "delay" for some aircraft is negative, which means they are assigned an RTA before the ETA. In average, the delay for the low traffic case-study is 75 s, while the maximum absolute delay is 341 s (almost 6 min). Overall, these delay values are relatively low.

Another interesting matter is the actual routes assignment. Depending on the entry point, one of the runways (i.e. north or south) would be more desirable for the incoming aircraft, as it would mean flying a shorter route. For aircraft starting the arrival procedure in

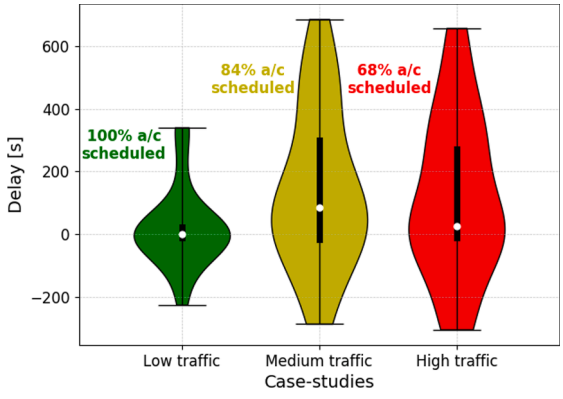


**Fig. 14.** Delays for the baseline case of the 3 traffic case-studies.

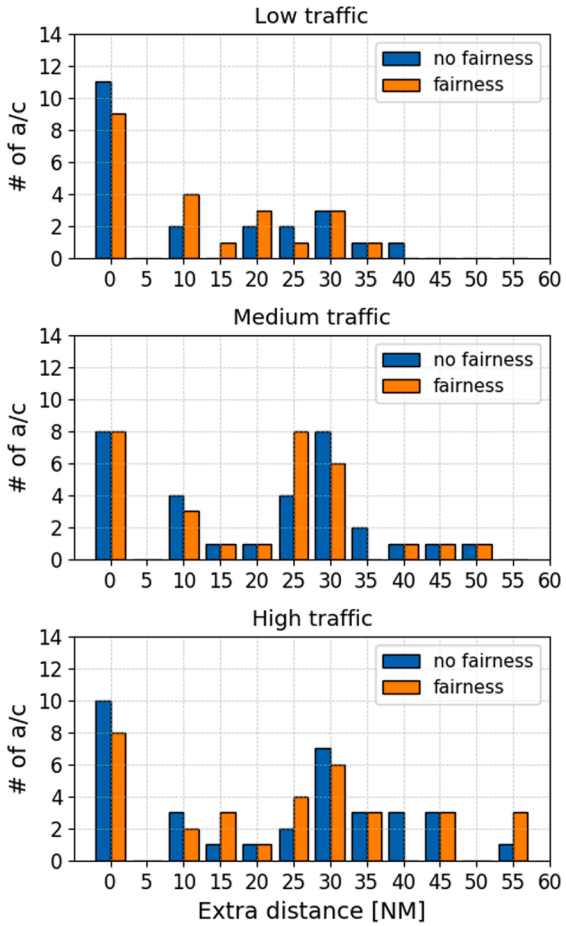


**Fig. 15.** Extra distance flown for the baseline case of the 3 traffic case-studies.

**Table 3**
Results for low traffic case-study.

| Flight ID | Entry point | Route | ETA (UTC) | RTA (UTC) | Delay (sec.) |
|---|---|---|---|---|---|
| 209912693 | ASPAT | 08 | 14:57:13 | 14:55:49 | −84 |
| 209903832 | KERAX | 05 | 14:57:58 | 14:57:58 | 0 |
| 209922177 | UNOKO | 10 | 14:59:41 | 15:00:28 | 47 |
| 209923238 | UNOKO | 05 | 15:04:23 | 15:04:23 | 0 |
| 209909575 | UNOKO | 05 | 15:10:58 | 15:10:58 | 0 |
| 209903416 | KERAX | 01 | 15:13:56 | 15:13:29 | −27 |
| 209918608 | ASPAT | 07 | 15:17:44 | 15:15:36 | −128 |
| 209919516 | EMPAX | 10 | 15:17:57 | 15:17:57 | 0 |
| 209920805 | UNOKO | 05 | 15:20:27 | 15:20:27 | 0 |
| 209922757 | KERAX | 05 | 15:25:17 | 15:25:17 | 0 |
| 209921846 | EMPAX | 10 | 15:29:59 | 15:29:59 | 0 |
| 209923949 | KERAX | 04 | 15:40:44 | 15:40:33 | −11 |
| 209921936 | KERAX | 04 | 15:46:35 | 15:42:50 | −225 |
| 209920383 | PSA | 04 | 15:45:08 | 15:44:56 | −12 |
| 209919813 | KERAX | 05 | 15:47:47 | 15:47:47 | 0 |
| 209920720 | ASPAT | 05 | 15:48:37 | 15:50:10 | 93 |
| 209922778 | EMPAX | 10 | 15:46:37 | 15:52:18 | 341 |
| 209923810 | UNOKO | 06 | 15:48:50 | 15:54:29 | 339 |
| 209924354 | KERAX | 10 | 15:53:14 | 15:56:40 | 206 |
| 209924874 | ASPAT | 08 | 16:03:45 | 16:02:21 | −84 |
| 209921663 | EMPAX | 05 | 16:04:39 | 16:04:34 | −5 |
| 209924577 | UNOKO | 10 | 16:05:47 | 16:06:40 | 53 |

KERAX, ROLIS and UNOKO route 05 is the shortest one, while for aircraft starting in PSA, ASPAT, PETIX or EMPAX route 10 would be the shortest one (Fig. 8). Table 3 shows how half of the aircraft are assigned the shortest possible route (either 10 or 05 depending on the entry point). The rest are assigned shortcuts that increase the total distance flown, as shown in Fig. 15. Appendix A presents two tables with the same format as Table 3 for the medium and high traffic case-studies, showing only those aircraft successfully scheduled.

### 4.4. Model enhancement results

As it has been explained in Section 4.2, the 100% of the incoming traffic was only scheduled for the low traffic case-study, while losses of separation were found in the medium and high traffic cases that were not possible to solve with neutral CDOs and the available set of routes. This section analyzes the effect of changing certain parameters, as explained in Section 3.5. These are the availability of additional tromboning shortcuts, the entry time distribution, the fairness strategy and the time separation. Table 4 shows the percentage of aircraft scheduled, average delay and maximum delay per case-study. Fig. 16 shows the delay distribution for all the case-studies and for all the enhancements made to the model except for the time separation analysis, which is shown in Fig. 17.

As it can be observed, the number of aircraft successfully scheduled increases in those case-studies where there is a change in the entry time. Dispersion also decreases, and delay is reduced. However, in the high traffic case-study it is still not possible to schedule the totality of the aircraft, even with a variation in the entry time of $\pm 5$ min there is still one aircraft that cannot be scheduled. The traffic order at the entry point is a very significant factor when scheduling the aircraft and in this case it was impossible to keep a minimum time separation between this remaining aircraft and the rest of the arriving traffic if neutral CDOs are flown. However, flying conventional descents or powered CDOs could help in this case. Nonetheless, it is worth noting the fact that by slightly modifying the entry time of the arriving aircraft it is possible to greatly increase the number of neutral CDOs that can be flown, even with high traffic loads.

Regarding those case-studies where additional shortcuts are added to the tromboning, although it is true that the delay is slightly reduced, it is not enough to ensure the minimum time separation between all aircraft throughout the procedure when the traffic density is high.

When fairness is considered, it can be observed that in all case-studies the average delay increases. In the low and high traffic case-studies, the maximum delay remains almost the same, while in the medium traffic case-study it decreases approximately by 1 min.

In general, due to the modification of the cost function, aircraft with a higher delay than average have now a lower delay, while aircraft that had a very low delay have now experienced some increase in the delay. However, some of the aircraft still have the same assigned delay due to the separation constraint; one such example is the aircraft which was assigned the highest delay in the high traffic case-study; as it can be seen in Table 4, the maximum delay for the high traffic scenario is the same in both cases.

**Table 4**
Model enhancement results.

| Traffic case-study | Enhancement case | % a/c scheduled | Avg. delay (seconds) | Max. delay (seconds) |
|---|---|---|---|---|
| Low | baseline | 100% | 75 | 341 |
| Low | $\pm 2'$ | 100% | 58 | 234 |
| Low | $\pm 5'$ | 100% | 53 | 296 |
| Low | additional shortcuts | 100% | 70 | 355 |
| Low | Fairness | 100% | 89 | 340 |
| Low | $t_{sep} + 20s$ | 100% | 113 | 556 |
| Low | indep. runways | 100% | 29 | 259 |
| Medium | baseline | 84% | 213 | 685 |
| Medium | $\pm 2'$ | 100% | 142 | 721 |
| Medium | $\pm 5'$ | 100% | 101 | 488 |
| Medium | additional shortcuts | 84% | 209 | 685 |
| Medium | Fairness | 84% | 222 | 622 |
| Medium | $t_{sep} + 20s$ | 71% | 123 | 364 |
| Medium | indep. runways | 84% | 64 | 317 |
| High | baseline | 68% | 203 | 657 |
| High | $\pm 2'$ | 76% | 77 | 277 |
| High | $\pm 5'$ | 98% | 137 | 488 |
| High | additional shortcuts | 68% | 150 | 558 |
| High | Fairness | 68% | 222 | 657 |
| High | $t_{sep} + 20s$ | 60% | 142 | 389 |
| High | indep. runways | 72% | 99 | 643 |

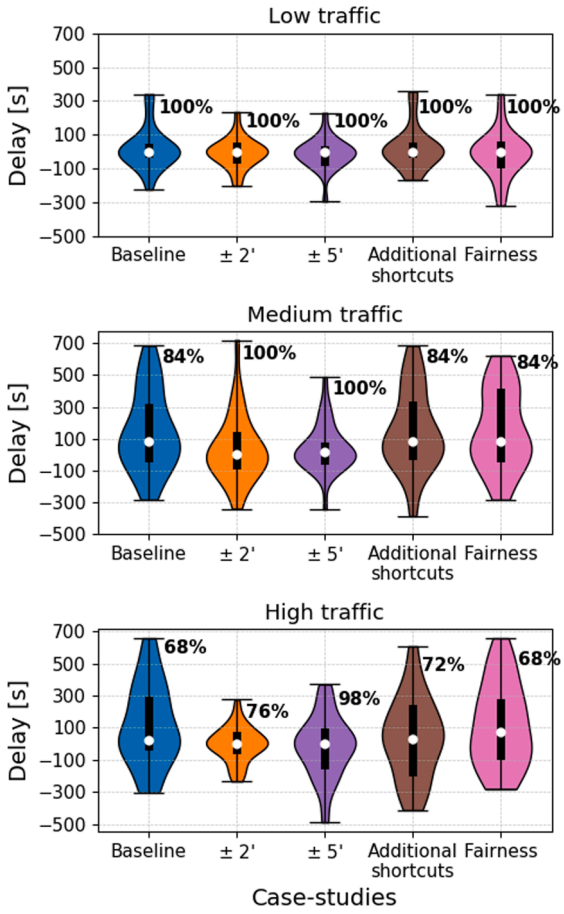


**Fig. 16.** Delay distribution and percentage of aircraft scheduled for the model enhancement.

Fig. 15 shows the extra distance flown by the aircraft to meet the assigned RTA with and without fairness considered in the delay assignment. It can be observed how some of the aircraft that before were assigned the shortest route (extra distance equal to 0 NM) are now assigned longer routes. For instance, in the low traffic case-study, the number of aircraft flying the shortest route is decreased by 2. On the other hand, some of the aircraft that were assigned longer routes before the modification, are flying shorter ones now, like the aircraft that was flying 40 extra NM in the low traffic case-study, which is no longer present in that distance range.

When considering changes in the minimum time separation between aircraft, big variations can be observed in both the number of aircraft scheduled and the average and maximum delay values (Table 4). In the low traffic case-study, the number of aircraft scheduled remains 100%; however, having a higher time separation translates into a higher delay dispersion, with both higher maximum and average delays (Fig. 17).

For the medium and high traffic case-studies, the situation is different, as not all aircraft are scheduled. The higher the time separation the lower the number of aircraft scheduled. In both case-studies, it can be observed that the delay decreases when the minimum separation is higher. When the separation increases, less aircraft can be scheduled and those which end up being scheduled require lower delays, as they can use the 'room' left by the non-scheduled aircraft. However, the entry time distribution may have a big effect in this case. Furthermore, the delay dispersion decreases.

Finally, if independent runways are considered, the results greatly improve, with lower average and maximum delays for all case-studies (Table 4, Fig. 17). However, the number of aircraft scheduled remains almost equal for all case-studies, with a slight increase in the high traffic scenario. Once again, it can be concluded that the traffic order at the entry point has a big effect in the number of aircraft that can be scheduled.

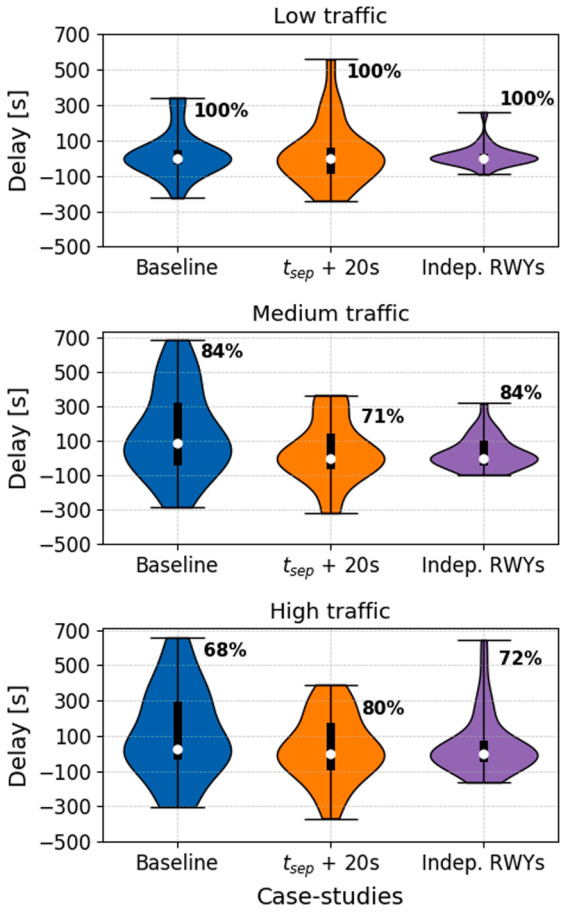


**Fig. 17.** Delay distribution and percentage of aircraft scheduled for a higher separation minima and for independent runways.

## 5. Conclusions

This paper proposed to sequence traffic in the terminal maneuvering area (TMA) by means of 4D closed-loop instructions, based on current tromboning procedures, enabling aircraft to fly continuous descent operations (CDO) from cruise level to a given metering fix. Results show that, after assigning required times of arrival (RTAs) and routes to every arriving aircraft when still in cruise, it is possible to ensure that a high percentage of them will perform neutral CDOs (with idle thrust and no speed-brakes usage), guaranteeing at the same time a safe separation between aircraft throughout the whole descent.

In this work, the objective was to maximize the number of aircraft performing neutral CDOs. However, this kind of operations involve aircraft having a more limited time window in the metering fix than in conventional descends or in powered CDOs (where both thrust and speed-brakes usage is allowed). As a result, the scheduling process becomes more challenging. Furthermore, the aircraft entry distribution is also a key factor affecting the feasibility of the solution proposed. Better distributions where aircraft arrive with enough separation at the entry points would represent an increase in the number of neutral CDOs performed and, therefore, an improvement in the efficiency of the operations.

While the concept of operations proposed in this paper works properly for low traffic scenarios, it could be concluded that in some cases, in airports or time periods with high traffic loads, it might be necessary to reformulate it. Basically, it would be worth investigating the possibility of establishing the communication between the arriving aircraft and the ATC even before arriving at the E-TMA. As it has been shown, gaining or losing 5 min in the en-route phase, just before entering the E-TMA, would avoid a lot of separation losses. Furthermore, other conflicts could also be avoided by gaining or losing time during the cruise section between the E-TMA entry point and the top of descent. Finally, due to the current computational times, the communication between the aircraft and the ATC might need to be established before the E-TMA too. Nonetheless, in this work the results were generated with a very simple prototype; there are several ways in which it could be improved: several tasks could be parallelized, a more efficient code could be written and a more powerful computer or server could be used.

The concept of operations proposed in this paper should be understood as an “interim” solution between the current operations and more futuristic approaches to the same problem with the TBO concepts deployed to its limits. In this work, the objective was to take advantage of the most advanced arrival and approach procedures currently in operation (such as tromboning) while maximizing the

number of neutral CDOs performed, by negotiating a route and an RTA at a given metering fix. However, it would be impossible to deploy this solution in other types of procedures, such as Point Merge, STARs with very restrictive speed and altitude constraints or procedures that usually rely on intensive tactical radar vectoring. In these cases, neutral CDOs would be infeasible and the concept of operations presented in this paper would not be viable. In the specific case of the STARs with very restrictive constraints, it is assumed that in a future TBO environment some of these constraints could be removed in favor of RTAs in several waypoints for both arriving and departing traffic (Vilardaga and Prats, 2015) that would also allow the use of neutral CDOs. Furthermore, aircraft not equipped with the RTA technology could not benefit from the solution proposed in this paper and they should be given vector instructions from the ATC. However, in a full-deployed TBO environment, it is reasonable to assume that (almost) all aircraft would be equipped with this functionality.

Nevertheless, the solution proposed in this paper aligns with the trajectory based operations (TBO) concept, where more detailed data is expected to be shared by aircraft and airlines, such as the EPP (extended projected profile) or more detailed aircraft intents downlinked. Thus, it is expected to become a technical enabler towards future arrival manager (AMAN) systems, providing more automated and enhanced ground support to the ATCOs and allowing flights to perform more efficient descents. See for instance the work in Sáez et al. (2020), which does not focus on pre-defined arrival procedures, but proposes to generate dynamic arrival routes that adapt to the traffic demand.

## Declaration of Competing Interest

The authors declare that they have no known competing financial interests or personal relationships that could have appeared to influence the work reported in this paper.

## Appendix A. Baseline results

Tables 5 and 6 show the results for the aircraft successfully scheduled in the medium and high traffic baseline scenarios respectively.

For the medium traffic case, 31 aircraft were scheduled, which represents an 84% of the arriving aircraft during that time, while in the high traffic case 34 aircraft were scheduled, which represents a 68% of the arriving traffic.

**Table 5**
Results for medium traffic scenario.

| Flight ID | Entry point | Route | ETA (UTC) | RTA (UTC) | Delay (sec.) |
|---|---|---|---|---|---|
| 209901616 | UNOKO | 03 | 06:56:38 | 06:56:04 | −34 |
| 209905972 | UNOKO | 05 | 06:58:13 | 06:58:13 | 0 |
| 209905861 | KERAX | 09 | 06:59:20 | 07:00:14 | 54 |
| 209907338 | UNOKO | 10 | 07:08:50 | 07:04:38 | −252 |
| 209906369 | ASPAT | 10 | 07:10:12 | 07:07:15 | −177 |
| 209904895 | KERAX | 01 | 07:11:24 | 07:09:20 | −124 |
| 209901977 | KERAX | 04 | 07:16:16 | 07:11:31 | −285 |
| 209906786 | UNOKO | 05 | 07:13:34 | 07:13:34 | 0 |
| 209901604 | UNOKO | 10 | 07:16:06 | 07:15:37 | −29 |
| 209907498 | PSA | 06 | 07:16:22 | 07:17:43 | 81 |
| 209907734 | KERAX | 05 | 07:20:59 | 07:20:16 | −43 |
| 209908172 | KERAX | 02 | 07:20:17 | 07:22:21 | 124 |
| 209906547 | PSA | 04 | 07:17:31 | 07:24:48 | 437 |
| 209901559 | UNOKO | 09 | 07:25:06 | 07:26:50 | 104 |
| 209907708 | UNOKO | 07 | 07:24:24 | 07:29:05 | 281 |
| 209905137 | EMPAX | 05 | 07:24:05 | 07:31:46 | 461 |
| 209907807 | KERAX | 07 | 07:23:43 | 07:33:47 | 604 |
| 209905625 | EMPAX | 08 | 07:28:23 | 07:35:49 | 446 |
| 209908418 | KERAX | 10 | 07:36:40 | 07:38:05 | 85 |
| 209907380 | UNOKO | 04 | 07:39:08 | 07:40:06 | 58 |
| 209906733 | EMPAX | 06 | 07:40:17 | 07:42:12 | 115 |
| 209903091 | PSA | 07 | 07:46:30 | 07:44:52 | −98 |
| 209902050 | UNOKO | 05 | 07:41:37 | 07:46:54 | 317 |
| 209900481 | UNOKO | 01 | 07:45:32 | 07:49:08 | 216 |
| 209907033 | ASPAT | 05 | 07:47:57 | 07:51:32 | 215 |
| 209907121 | EMPAX | 05 | 07:44:16 | 07:53:46 | 570 |
| 209908891 | ASPAT | 05 | 07:52:24 | 07:55:47 | 203 |
| 209907163 | UNOKO | 06 | 07:46:25 | 07:57:50 | 685 |
| 209906791 | PSA | 09 | 07:52:13 | 07:59:57 | 464 |
| 209909054 | KERAX | 08 | 08:03:03 | 08:02:55 | −8 |
| 209909126 | UNOKO | 10 | 08:04:19 | 08:04:58 | 39 |

**Table 6**
Results for high traffic scenario.

| Flight ID | Entry point | Route | ETA (UTC) | RTA (UTC) | Delay (sec.) |
|---|---|---|---|---|---|
| 209921147 | KERAX | 04 | 16:54:05 | 16:49:01 | −304 |
| 209905779 | KERAX | 04 | 16:54:52 | 16:51:42 | −190 |
| 209924440 | KERAX | 05 | 16:53:43 | 16:53:43 | 0 |
| 209916195 | ASPAT | 10 | 16:55:44 | 16:55:44 | 0 |
| 209914280 | KERAX | 05 | 16:58:49 | 16:58:49 | 0 |
| 209904774 | KERAX | 01 | 17:06:36 | 17:06:39 | 3 |
| 209924901 | ASPAT | 08 | 17:13:18 | 17:08:43 | −275 |
| 209925944 | KERAX | 04 | 17:15:05 | 17:11:02 | −243 |
| 209906722 | KERAX | 05 | 17:13:35 | 17:13:13 | −22 |
| 209923488 | UNOKO | 01 | 17:10:34 | 17:15:21 | 287 |
| 209926911 | EMPAX | 10 | 17:17:41 | 17:17:41 | 0 |
| 209979722 | ASPAT | 03 | 17:13:53 | 17:19:41 | 348 |
| 209921346 | KERAX | 05 | 17:23:39 | 17:23:39 | 0 |
| 209926920 | PSA | 03 | 17:18:44 | 17:25:41 | 417 |
| 209926853 | KERAX | 08 | 17:17:55 | 17:28:24 | 629 |
| 209926587 | ASPAT | 07 | 17:30:58 | 17:31:26 | 28 |
| 209927424 | KERAX | 03 | 17:35:32 | 17:34:06 | −86 |
| 209927718 | KERAX | 05 | 17:36:52 | 17:36:52 | 0 |
| 209927556 | EMPAX | 07 | 17:35:07 | 17:38:55 | 228 |
| 209924578 | KERAX | 09 | 17:31:38 | 17:40:56 | 558 |
| 209926663 | UNOKO | 06 | 17:32:37 | 17:43:34 | 657 |
| 209927152 | PSA | 05 | 17:41:59 | 17:46:05 | 246 |
| 209924673 | UNOKO | 01 | 17:48:32 | 17:48:13 | −19 |
| 209926303 | UNOKO | 10 | 17:45:58 | 17:50:14 | 256 |
| 209927974 | KERAX | 05 | 17:56:58 | 17:52:17 | −281 |
| 209927560 | KERAX | 06 | 17:47:42 | 17:54:57 | 435 |
| 209924999 | ASPAT | 04 | 17:56:05 | 17:57:13 | 68 |
| 209925224 | PETIX | 04 | 17:53:08 | 17:59:48 | 400 |
| 209928111 | ASPAT | 05 | 17:59:00 | 18:02:26 | 206 |
| 209925155 | PETIX | 05 | 18:01:48 | 18:05:34 | 226 |
| 209927507 | UNOKO | 06 | 18:01:54 | 18:08:00 | 366 |
| 209927876 | UNOKO | 10 | 18:16:42 | 18:16:19 | −23 |
| 209927762 | APSAT | 04 | 18:18:02 | 18:18:23 | 21 |
| 209928341 | PSA | 05 | 18:19:22 | 18:20:58 | 96 |

## References


Airbus, 1998. Getting to grips with the cost index. Flight Operations Support and Line Assistance, Blagnac, France, Tech. Rep.

Beasley, J., Krishnamoorthy, M., Sharaiha, Y., Abramson, D., 2000. Scheduling aircraft landings – The static case. Transport. Sci. 34, 180–197.

Beasley, J., Krishnamoorthy, M., Sharaiha, Y., Abramson, D., 2011. Improved ant colony algorithm to solve the aircraft landing problem. Int. J. Comput. Theory Eng. 3 (2), 224–233.

Benheikh, G., Boukachour, J., El Hilali, A., El Khoukhi, F., 2009. Hybrid method for aircraft landing scheduling based on a Job Shop formulation. Int. J. Comput. Sci. Netowrk Sec. 9 (8), 78–88.

Bertsimas, D., Patterson, S.S., 1998. The air traffic flow management problem with enroute capacities. Oper. Res. 46 (3), 406–422.

Boursier, L., Favennec, B., Hoffman, E., Trzmiel, A., Vergne, F., Zeghal, K., 2007. Merging arrival flows without heading instructions. In: USA/Europe Air Traffic Management Research and Development Seminar, no. July, pp. 1–8.

Bryson, A.E., Ho, Y.-C., 1975. Applied Optimal Control: Optimization, Estimation, and Control. Taylor and Francis Group, New York, USA.

Clarke, J.P.B., Ho, N.T., Ren, L., Brown, J.A., Elmer, K.R., Zou, K.F., Hunting, C., McGregor, D.L., Shivashankara, B.N., Tong, K., Warren, A.W., Wat, J.K., 2004. Continuous descent approach: Design and flight test for Louisville international airport. J. Aircraft 41 (5), 1054–1066.

Dalmau, R., Prats, X., 2017. Controlled time of arrival windows for already initiated energy-neutral continuous descent operations. Transport. Res. Part C: Emerg. Technol. 85, 334–347.

Dalmau, R., Verhoeven, R., Gelder, N.D., Prats, X., 2016. Performance comparison between TEMO and a typical FMS in presence of CTA and wind uncertainties. In: IEEE/AIAA 35th Digital Avionics Systems Conference (DASC), Sacramento, USA.

Dalmau, R., Prats, X., Verhoeven, R., Bussink, F., Heesbeen, B., 2019. Comparison of various guidance strategies to achieve time constraints in optimal descents. J. Guidance Control Dyn. 42 (7).

de Boor, C., 1972. On calculating with B-splines. J. Approxim. Theory 6 (1), 50–62.

de Jong, P.M.A., van der Laan, J.J., Veld, A.C., van Paassen, M.M., Mulder, M., 2014. Wind-profile estimation using airborne sensors. J. Aircraft 51 (6), 1852–1863.

Delgado, L., Prats, X., 2012. En route speed reduction concept for absorbing air traffic flow management delays. J. Aircraft 49 (1), 214–224.

Delgado, L., Prats, X., 2013. Effect of wind on operating-cost-based cruise speed reduction for delay absorption. IEEE Trans. Intell. Transp. Syst. 14 (2), 918–927.

Erkelens, L., 2000. Research into new noise abatement procedures for the 21st century. In: AIAA Guidance, Navigation, and Control Conference and Exhibit, ser. Guidance, Navigation, and Control and Co-located Conferences. American Institute of Aeronautics and Astronautics, Denver, CO, 2000.

Eurocontrol, 2017. DDR2 Reference Manual for General Users 2.9.4.

Federal Aviation Administration, 2019. NextGen Implementation Plan 2018-19, Washington, D.C, Tech. Rep.

Fricke, H., Seiß, C., Herrmann, R., 2015. Fuel and Energy Benchmark Analysis of Continuous Descent Operations. In: USA/Europe Air Traffic Management Research and Development Seminar, vol. 23, no. ATC Quarterly Special Issue, Washington D.C., USA, pp. 83–108.

ICAO, 2020. Continuous Descent Operations (CDO) Manual-Doc 9931/AN/476. In: (ICAO), International Civil Aviation Organization, Montréal, Quebec, Canada, Tech. Rep.

ICAO, Doc 4444, 2016. Procedures for air navigation services - Air Traffic Management, 16th ed., Montréal, Quebec, Canada.

Ivanescu, D., Shaw, C., Tamvaclis, C., Kettunen, T., 2009. Models of air traffic merging techniques: evaluating performance of point merge. In: 9th AIAA Aviation Technology, Integration, and Operations (ATIO) Conference, Hilton Head, South Carolina.

Klooster, J.K., Amo, A.D., Manzi, P., 2009. Controlled time-of-arrival flight trials. In: 8th USA/Europe Air Traffic Management Research and Development Seminar, Napa, CA,.

Park, S.G., Dutta, P., Menon, P.K., June 2017. Optimal trajectory option sets for in-flight climb-descend trajectory negotiations. In: 17th AIAA Aviation Technology, Integration, and Operations Conference (ATIO). AIAA, Denver, CO.

Pawełek, A., Lichota, P., Dalmau, R., Prats, X., 2019. Fuel-efficient trajectories traffic synchronization. J. Aircraft 56 (2), 481–492.

Poles, D., Nuic, A., Mouillet, V., 2010. Advanced aircraft performance modelling for ATM: Analysis of BADA model capabilities. In 29th Digital Avionics Systems Conference. Brétigny-sur-Orge (France): EUROCONTROL.

Prats, X., Dalmau, R., Verhoeven, R., Bussink, F., 2017. Human-in-the-loop performance assessment of optimized descents with time constraints. results from full motion flight simulation and a flight testing campaign. In: Proceedings of the 12th USA/Europe Air Traffic Management Research and Development Seminar. Seattle, WA (USA): Eurocontrol and FAA.

Sadovsky, A.V., Windhorst, R.D., 2019. A scheduling algorithm compatible with a distributed management of arrivals in the national airspace system. In: Proceedings of the 38th IEEE/AIAA Digital Avionics Systems Conference (DASC). IEEE and AIAA.

Sáez, R., Dalmau, R., Prats, X., 2018. Optimal assignment of 4D close-loop instructions to enable CDOs in dense TMAs. In: Proceedings of the 37th IEEE/AIAA Digital Avionics Systems Conference (DASC). IEEE and AIAA.

Sáez, R., Prats, X., Polishchuk, T., Polishchuk, V., Schmidt, C., 2020. Automation for separation with CDOs: dynamic aircraft arrival routes. AIAA J. Air Transport. 28 (4).

Samà, M., D'Ariano, A., D'Ariano, P., Pacciarelli, D., 2014. Optimal aircraft scheduling and routing at a terminal control area during disturbances. Transport. Res. Part C: Emerg. Technol. 47 (1), 61–85.

SESAR Joint Undertaking, 2015. 'European ATM Master Plan. The roadmap for delivering high performing aviation for Europe, Brussels, Tech. Rep.

SKYbrary, 2020. ICAO Wake Turbulence Category, https://www.skybrary.aero/index.php/ICAO_Wake_Turbulence_Category, Accessed: 2020-05-12.

Sprong, K., Haltli, B., DeArmon, J., Bradley, S., 2005. Improving flight efficiency through terminal area rnav. In: 6th USA/Europe Air Traffic Managament Research and Development Seminar. Eurocontrol and FAA.

Takeichi, N., Inami, D., 2010. Arrival-time controllability of tailored arrival subjected to flight-path constraints. J. Aircraft 47 (6), 2021–2029.

Vadlamani, S., Seyedmohsen, H., 2014. A novel heuristic approach for solving aircraft landing problem with single runway. J. Air Transport Manage. 40, 144–148.

Vilardaga, S., Prats, X., Dec 2015. Operating cost sensitivity to required time of arrival commands to ensure separation in optimal aircraft 4d trajectories. Transport. Res. Part C: Emerg. Technol. 61, 75–86.

Warren, A., Tong, K., 2002. "Development of continuous descent approach concepts for noise abatement. In: IEEE/AIAA 21st Digital Avionics Systems Conference (DASC), Irvine, CA.

Zelinksi, S.J., Jung, J., 2015. Arrival scheduling with shortcut path options and mixed aircraft performance. In: Proceedings of the 11th USA/Europe Air Traffic Management Research and Development Seminar. Lisbon, Portugal: Eurocontrol and FAA.